



Calhoun: The NPS Institutional Archive

Theses and Dissertations

Thesis Collection

1992-12

**Comparison calibration of piezoresistive
microphones for acoustic power measurements**

Stockermans, Ron J.

Monterey, California. Naval Postgraduate School

<http://hdl.handle.net/10945/23572>



Calhoun is a project of the Dudley Knox Library at NPS, furthering the precepts and goals of open government and government transparency. All information contained herein has been approved for release by the NPS Public Affairs Officer.

**Dudley Knox Library / Naval Postgraduate School
411 Dyer Road / 1 University Circle
Monterey, California USA 93943**

<http://www.nps.edu/library>



REPORT DOCUMENTATION PAGE

1a Report Security Classification Unclassified		1b Restrictive Markings	
2a Security Classification Authority		3 Distribution Availability of Report: Approved for public release; distribution is unlimited.	
2b Declassification/Downgrading Schedule		5 Monitoring Organization Report Number(s)	
4 Performing Organization Report Number(s)		7a Name of Monitoring Organization Naval Research Laboratory	
6a Name of Performing Organization Naval Postgraduate School	6b Office Symbol (If Applicable) 33	7b Address (city, state, and ZIP code) Washington, DC 20375-5000	
6c Address (city, state, and ZIP code) Monterey, CA 93943-5000		9 Procurement Instrument Identification Number	
8a Name of Funding/Sponsoring Organization NPS	8b Office Symbol (If Applicable)	10 Source of Funding Numbers	
8c Address (city, state, and ZIP code)		Program Element Number	Project No
		Task No	Work Unit Accession No
11 Title (Include Security Classification) COMPARISON CALIBRATION OF PIEZORESISTIVE MICROPHONES FOR ACOUSTIC POWER MEASUREMENTS			
12 Personal Author(s) Ron J. Stockermans			
13a Type of Report Master's Thesis	13b Time Covered From To	14 Date of Report (year, month, day) December 1992	15 Page Count 79
16 Supplementary Notation The views expressed in this thesis are those of the author and do not reflect the official policy or position of the Department of Defense or the U.S. Government.			
17 Cosati Codes Field Group Subgroup		18 Subject Terms (continue on reverse if necessary and identify by block number) microphone, calibration, closed volume, piezoresistive, piezoelectric, condenser	
19 Abstract (continue on reverse if necessary and identify by block number) A calibration of two Endevco piezoresistive microphones was carried out under static and dynamic pressures. The dynamic pressure calibrations were done by comparison with a B&K condenser microphone. The calibration was carried out in a small closed volume in air and helium. In helium, the closed volume was pressurized to atmospheric pressure and then 10 Atm. The dynamic calibration would determine the "flatness" of the calibration curve, as well as determine a sensitivity value over the range of frequencies used. The results showed that the calibration curve for the piezoresistive microphones are flat from static pressures to about 300 Hz and then begin to fall off. The value of the sensitivity of the "flat" region of the calibration curve for one microphone was within 0.4% of the value for sensitivity calculated under the static pressure calibration. For the other microphone the static and dynamic sensitivities were within 1.3% of each other. Thus, the static calibration of one microphone may be used under dynamic conditions with a less than 1% error while using the other microphone similarly will produce an error of greater than 1%.			
20 Distribution/Availability of Abstract <input checked="" type="checkbox"/> unclassified/unlimited <input type="checkbox"/> same as report <input type="checkbox"/> DTIC users		21 Abstract Security Classification Unclassified	
22a Name of Responsible Individual Tom J. Hofler		22b Telephone (Include Area code) (408) 646-2420	22c Office Symbol PH/Hf

T258757

Approved for public release; distribution is unlimited

**COMPARISON CALIBRATION OF PIEZORESISTIVE MICROPHONES
FOR ACOUSTIC POWER MEASUREMENTS**

by

Ron J Stockermans
Captain, Canadian Forces
B.Eng., Royal Military College of Canada, 1982

Submitted in partial fulfillment of the requirements for the degree of
MASTER OF SCIENCE IN ENGINEERING ACOUSTICS

from the

NAVAL POSTGRADUATE SCHOOL

December 1992

Anthony A. Atchley/Chairman
Engineering Acoustics Academic Committee

ABSTRACT

A calibration of two Endevco piezoresistive microphones was carried out under static and dynamic pressures. The dynamic pressure calibrations were done by comparison with a B&K condenser microphone. The calibration was carried out in a small closed volume in air and helium. In helium, the closed volume was pressurized to atmospheric pressure and then 10 Atm. The dynamic calibration would determine the "flatness" of the calibration curve, as well as determine a sensitivity value over the range of frequencies used. The results showed that the calibration curve for the piezoresistive microphones are flat from static pressures to about 300 Hz and then begin to fall off. The value of the sensitivity of the "flat" region of the calibration curve for one microphone was within 0.4% of the value for sensitivity calculated under the static pressure calibration. For the other microphone the static and dynamic sensitivities were within 1.3% of each other. Thus, the static calibration of one microphone may be used under dynamic conditions with a less than 1% error while using the other microphone similarly will produce an error of greater than 1%.

110515
57315
c.1

TABLE OF CONTENTS

I. INTRODUCTION	1
II. THEORY.....	3
A. COMPARISON CALIBRATION.....	3
1. Static Calibration.....	3
2. Dynamic Comparison Calibration.....	4
3. Cavity Effects	6
B. MICROPHONE THEORY.....	8
1. Piezoresistive microphone	8
2. Piezoelectric quartz microphone.....	9
3. Condenser microphone.....	11
III. APPARATUS	14
A. MICROPHONES	14
1. Piezoresistive Microphone.....	14
2. Piezoresistive Microphone Housing.....	15
3. Piezoelectric Quartz Microphone.....	16
4. Condenser Microphone	17
B. DYNAMIC PRESSURE VESSEL.....	18
C. MEASUREMENT EQUIPMENT.....	20
1. Static Calibration Apparatus	20
2. Dynamic Calibration Apparatus	21
a. Piezoresistive Microphone Installed on Apparatus.....	21
b. Condenser Microphone Installed on Apparatus	24
3. Condenser Microphone Calibration Apparatus.....	24
IV. THE STATIC PRESSURE TEST	27
A. EXPERIMENT.....	27
B. RESULTS.....	28
V. THE DYNAMIC PRESSURE TEST.....	33
A. PIEZORESISTIVE MICROPHONE FREQUENCY RESPONSE.....	33
1. Fluid Medium: Low Pressure Air	33
2. Fluid Medium: Low Pressure Helium	34
3. Fluid Medium: High Pressure Helium.....	34
B. CONDENSER MICROPHONE FREQUENCY RESPONSE	34
1. Fluid Medium: Low Pressure Air	34

2.	Fluid Medium: Low Pressure Helium	35
C.	RESULTS	35
1.	Piezoresistive Microphone Frequency Response	35
a.	Low Pressure Air	36
b.	Low Pressure Helium	37
c.	High Pressure Helium.....	42
2.	Condenser Microphone Frequency Response.....	46
a.	Low Pressure Air	46
b.	Low Pressure Helium	47
3.	Condenser Microphone Calibration.....	53
4.	Piezoresistive Microphone Calibration	54
VI	CONCLUSIONS	59
	APPENDIX A: Schematic Diagram Of Piezoresistive Microphone Preamplifier.....	63
	REFERENCES	66
	INITIAL DISTRIBUTION LIST	68

LIST OF TABLES

TABLE 6.1. SUMMARY OF RESULTS	59
-------------------------------------	----

LIST OF FIGURES

Figure 2.1 Wheatstone Bridge Diagram of the Piezoresistive Microphone.....	8
Figure 2.2 Model and Electrical Equivalent Circuit of the Piezoelectric Quartz Microphone.	10
Figure 2.3 Electrical Schematic Diagram of the Condenser Microphone.	12
Figure 3.1 Cut-away view of the Piezoresistive Microphone Housing.....	15
Figure 3.2 Mounting Diagram of the Condenser Microphone.	17
Figure 3.3 Dynamic Pressure Vessel.	19
Figure 3.4 Static Calibration Apparatus	20
Figure 3.5 Pressure Head Calibration Chart	22
Figure 3.6 Dynamic Calibration Apparatus	23
Figure 3.7 Condenser Microphone Calibration Apparatus	25
Figure 3.8 Pistonphone Calibration Chart.....	26
Figure 4.1 Static Calibration of Piezoresistive Microphone #1 for Data Points below ± 2 psi.....	28
Figure 4.2 Static Calibration of Piezoresistive Microphone #1 for Data Points below ± 1 psi.....	29
Figure 4.3 Static Calibration of Piezoresistive Microphone #1 for Data Points below ± 0.5 psi.....	30
Figure 4.4 Static Calibration of Piezoresistive Microphone #2 for Data Points below ± 1 psi.....	31
Figure 5.1 Frequency response of the piezoresistive microphone #1 with respect to the frequency response of the piezoelectric quartz microphone in low pressure air.....	36
Figure 5.2 Frequency response of the piezoresistive microphone #2 with respect to the frequency response of the piezoelectric quartz microphone in low pressure air.....	37
Figure 5.3 Frequency response of the piezoresistive microphone #1 with respect to the frequency response of the piezoelectric quartz microphone in low pressure helium.....	38
Figure 5.4 Frequency response of the piezoresistive microphone #2 with respect to the frequency response of the piezoelectric quartz microphone in low pressure helium.....	39
Figure 5.5 The "pattern factor" with piezoresistive microphone #1. Or, frequency response of the piezoresistive microphone #1 in low pressure air with respect to the frequency response of the piezoresistive microphone #1 in low pressure helium.....	40
Figure 5.6 The "pattern factor" with piezoresistive microphone #2. Or, frequency response of the piezoresistive microphone #2 in low pressure air with respect	

to the frequency response of the piezoresistive microphone #2 in low pressure helium.....	41
Figure 5.7 Frequency response of the piezoresistive microphone #1 with respect to the frequency response of the piezoelectric quartz microphone in high pressure helium.....	42
Figure 5.8 Frequency response of the piezoresistive microphone #2 with respect to the frequency response of the piezoelectric quartz microphone in high pressure helium.....	43
Figure 5.9 Comparison of the Frequency response of the piezoresistive microphone #1 in low pressure helium reference to its response in high pressure helium.....	44
Figure 5.10 Comparison of the frequency response of the piezoresistive microphone #2 in low pressure helium reference to its response in high pressure helium.....	45
Figure 5.11 Frequency response of the 1/4" condenser microphone with respect to the frequency response of the piezoelectric quartz microphone in low pressure air.....	46
Figure 5.12 Frequency response of the 1/4" condenser microphone with respect to the frequency response of the piezoelectric quartz microphone in low pressure helium.....	48
Figure 5.13 The "pattern factor" with the condenser microphone.....	49
Figure 5.14 Frequency response of the piezoresistive microphone #1 with respect to the frequency response of the 1/4" condenser microphone in low pressure air.....	51
Figure 5.15 Frequency response of the piezoresistive microphone #2 with respect to the frequency response of the 1/4" condenser microphone in low pressure air.....	52
Figure 5.16 Newly calibrated manufacturers calibration chart for the 1/4" condenser microphone	54
Figure 5.17 Calibration curve for the piezoresistive microphone #1.....	56
Figure 5.18 Calibration curve for the piezoresistive microphone #2.....	57
Figure 6.1 Absolute calibration of the piezoresistive microphone #1.....	60
Figure 6.2 Absolute calibration of the piezoresistive microphone #2.....	61
Figure A.1 Schematic Diagram Of Piezoresistive Microphone Preamplifier, Drawing 1 of 3.....	63
Figure A.2 Schematic Diagram Of Piezoresistive Microphone Preamplifier, Drawing 2 of 3.....	64
Figure A.3 Schematic Diagram Of Piezoresistive Microphone Preamplifier, Drawing 3 of 3.....	65

ACKNOWLEDGEMENTS

I would like to thank Dr. Tom Hofler, for his guidance with my thesis and Lt Glenn Miller, USN, for his humour and his perspective on school. I would also like to thank my wife, Cathy, for her support and encouragement. She has patiently endured the past two and a half years of my studies, and I am deeply grateful to her.

I. INTRODUCTION

Current research in Thermoacoustic Refrigerators requires accurate measurement of the acoustic power of the refrigerator's driver in order to determine the intrinsic acoustic-to-thermal efficiency of the refrigerator. The acoustic power can be determined by knowing the electric power delivered to the driver and its efficiency, but driver efficiency is not constant with respect to typical variations in operating conditions. Thus, a way is needed to directly measure the acoustic power output of the driver.

Hofler describes just such a method [Ref. 1] where, in a closed helium filled vessel, the pressure field at the driver and the acceleration of the driver itself are measured and the results are combined to obtain acoustic power. In determining the acoustic power of the driver the dominant source of uncertainty at moderate drive levels comes from the pressure transducer sensitivity. The pressure transducer sensitivity, in fact, appears squared in the expression for power, and so the uncertainty in the power measurement is twice that of the uncertainty in the sensitivity of the pressure transducer. Since we want to measure the acoustic power of the driver to within $\pm 2\%$ accuracy, the uncertainty of the sensitivity of the pressure transducer must be less than $\pm 1\%$. In order to obtain these accurate results, an accurate calibration of the pressure transducer which measures the acoustic pressure field must be made. The most expedient method of calibrating this pressure transducer is by comparison to a standard microphone. Since the standard microphone must have a calibration at least as accurate as the pressure transducer, the object of this thesis then, is to calibrate this standard microphone to within a $\pm 1\%$ level of uncertainty.

To accomplish this aim, I am using two piezoresistive microphones [Ref. 2] as the standard microphones to be calibrated. Two microphones are being calibrated since it is always useful to have two standard microphones in the laboratory instead of one. Since the

design of the piezoresistive microphone is such that it responds equally well to both static and dynamic pressures, I have conducted experiments to determine if the sensitivity of the microphone is the same at static and dynamic pressures up to 1 kHz. Typical thermoacoustic refrigerators operate at 600 Hz or below. The method of calibration I used in this thesis is the comparison method where both a high quality condenser microphone [Ref. 3] and a high quality static pressure gauge were used as the references. A dynamic calibration was carried out inside an enclosed cavity where a piezoelectric quartz microphone is permanently mounted to be used as a interim reference microphone. The desired dynamic calibration is determined by first generating the frequency response of the piezoresistive microphone reference to the piezoelectric microphone and comparing that to the frequency response of the condenser microphone reference to the piezoelectric microphone. This result is then extrapolated to zero frequency and compared to the results of the static calibration test. An advantage of the piezoresistive microphone is that it can be calibrated statically. If a high degree of "flatness" of the frequency response can be established below 600 Hz, for the particular transducers used in this thesis, then static calibration may be sufficient for future re-calibrations. Generally, the static calibration can be done more quickly and more accurately.

This thesis is organized to first present the calibration theory I employed as well as the theory behind the three different types of microphones used. Next, a chapter containing a description of the apparatus used during this thesis is provided and an explanation its operation. This is followed by a chapter on the static calibration of the standard microphone and the results. The next chapter concerns the dynamic or frequency dependent calibration of the standard microphone and the results. To conclude the thesis, I have included a summary of the experiments I have conducted and their results.

II. THEORY

A. COMPARISON CALIBRATION

The purpose of this thesis is to provide a calibration of two piezoresistive microphones using two separate, independent comparison techniques to ensure confidence in the results of these experiments. The first technique is a static calibration test, and the second is a dynamic calibration test. The dynamic calibration consists of two parts; the first is where a microphone of known sensitivity is used as the reference microphone to determine the "flatness" of the frequency response of the two piezoresistive microphones, and the second is an absolute calibration of the reference microphone at a single frequency (251.2 Hz). If we can determine that the frequency response of the two piezoresistive microphones is constant or "flat", then we may directly compare the the calibration value measured at 251.2 Hz to the static calibration value in order to confirm that the static value is indeed accurate.

The theory behind these techniques are described in detail in this chapter. The frequency range used in the dynamic experiments was from 1 to 1000 Hz. This range was selected to span the range of interest of acoustic power measurements (between 400 and 600 Hz) at the high end of the range, as well as to approach reasonably close to static pressures at the low end of the range.

1. Static Calibration

The static calibration measures the sensitivity of a microphone under static conditions. The procedure for this technique goes as follows: Microphone X of unknown sensitivity has a known pressure, P , applied to one side of its sensing area and its electrical response in volts, V , is recorded as a function of that pressure for several values above and below ambient pressure. At each increment of pressure, the sensitivity is given by

$$M_X = \frac{V}{P} \tag{2.1}$$

By plotting the data pairs as V vs P and accounting for any preamplifier gain as appropriate, the slope of the line will determine the microphone static sensitivity, M_X .

2. Dynamic Comparison Calibration

The procedure for this technique, as described by Kinsler *et. al.* [Ref. 4], goes as follows: Microphone X of unknown sensitivity, M_X , is placed in a sound field and its electrical response, V_X , is recorded as a function of frequency. Then, microphone A of known sensitivity, M_A , and with dimensions similar to X is placed in the same sound field and oriented in the same manner as microphone X. V_A , the electrical response of microphone A, is recorded as a function of the same frequencies as microphone X. At each frequency, the sensitivity is given by

$$M_X = M_A \frac{V_X}{V_A} \quad (2.2)]$$

The actual dynamic comparison calibration experiments are carried out in an enclosed cylindrical cavity. This cavity contains a hemispherical driver at one end of the cavity and at the other end, either microphone X, the piezoresistive microphone, or microphone A, the condenser microphone. Since both microphones cannot be located in the cavity at the same time a piezoelectric quartz microphone, called microphone Q, is permanently mounted in the cavity wall and is used as the interim reference microphone.

When the experiments are carried out, the piezoresistive microphone is mounted in the cylindrical cavity first and its frequency response is recorded with reference to the piezoelectric quartz microphone. If the cavity is sufficiently small compared to a wavelength, then the pressure is constant everywhere in the cavity and thus equation 2.2 can be used. That is, the ratio $\frac{V_X}{V_Q}$ is recorded at several frequencies from 1 to 1000 Hz. At each frequency, the sensitivity is given by

$$M_X = M_Q \frac{V_X}{V_Q} \quad (2.3)$$

The same frequency response operation is carried out again with the condenser microphone mounted to the cylindrical cavity. Similarly, the ratio $\frac{V_A}{V_Q}$ is recorded at the same frequencies from 1 to 1000 Hz. At each frequency, the sensitivity is given by

$$M_A = M_Q \frac{V_A}{V_Q} \quad (2.4)$$

As long as the electrical response is recorded for the same frequencies in both tests, then from equations 2.3 and 2.4 we can say

$$\frac{M_X}{M_A} = \frac{\left(M_Q \frac{V_X}{V_Q} \right)}{\left(M_Q \frac{V_A}{V_Q} \right)} = \frac{\left(\frac{V_X}{V_Q} \right)}{\left(\frac{V_A}{V_Q} \right)} \quad (2.5)$$

or,

$$M_X = M_A \frac{\left(\frac{V_X}{V_Q} \right)}{\left(\frac{V_A}{V_Q} \right)} \quad (2.6)$$

or,

$$20 \text{ Log } M_X = 20 \text{ Log } M_A + 20 \text{ Log } \frac{V_X}{V_Q} - 20 \text{ Log } \frac{V_A}{V_Q} \quad (2.7)$$

where $20 \text{ Log } M_X$ is the sensitivity, in dB, of the piezoresistive microphone; $20 \text{ Log } M_A$ is the known sensitivity, in dB, of the condenser microphone; $20 \text{ Log } \frac{V_X}{V_Q}$ is the ratio of frequency responses, in dB, of the piezoresistive to the piezoelectric quartz microphones; and $20 \text{ Log } \frac{V_A}{V_Q}$ is the ratio of frequency responses, in dB, of the condenser to the

piezoelectric quartz microphones. The values $20 \text{ Log } \frac{V_X}{V_Q}$ and $20 \text{ Log } \frac{V_A}{V_Q}$ are useful quantities since they are easily determined with the electronic measurement equipment that is available.

Using this technique, the sensitivity of the the interim piezoelectric quartz microphone is cancelled out and so its properties become unimportant quantities for this experiment.

2. Cavity Effects

An important consideration when using an enclosed cavity for calibrations is the resonant or modal effects of the cavity. Since the piezoelectric quartz microphone and the microphone under test are not co-located inside the cavity, some acoustic pressure amplitude differences between them can be expected especially at higher frequencies where the wavelength approaches the cavity dimensions. These pressure amplitude differences or cavity effects will be reflected in the frequency response data obtained during the tests. However, by cancelling out the response from the piezoelectric quartz microphone, the effect of these cavity dependent responses will, in the final analysis, also be cancelled out. Since the piezoresistive microphones and the condenser microphone are, in effect, co-located, they will each in turn see the same acoustic pressure amplitude variation relative to the piezoelectric quartz microphone and so this variation cancels out from equation 2.6.

Beranek [Ref. 5] describes another method that was used in this experiment to measure the cavity effects. The method requires that a gas with a higher sound speed be injected into the cavity. Helium is ordinarily used for this purpose since it is inert and has a speed of sound that is roughly three times faster than that of air. Since

$$f_{o_{\text{helium}}} = \frac{c_{\text{helium}}}{\lambda} \quad (2.8)$$

and since,
$$c_{\text{helium}} \doteq 3c_{\text{air}} \quad (2.9)$$

then

$$f_{o_{\text{helium}}} \doteq 3 \frac{c_{\text{air}}}{\lambda} = 3f_{o_{\text{air}}} \quad (2.10)$$

where $f_{o_{\text{helium}}}$ and $f_{o_{\text{air}}}$ are some resonant frequency of the cavity in helium and air respectively; and c_{helium} and c_{air} are the speeds of sound in helium and air respectively. Thus, resonant effects of the cavity will occur at frequencies roughly three times higher with helium than if air were the fluid medium. Any resonance effects occurring in air near the frequency range of interest will, in helium, be shifted to a higher frequency and out of the range of interest.

Another way of looking at the use of helium is the result one gets when the relative response of the piezoresistive and quartz microphones in helium is compared to their response in air in a ratio such as:

$$F = \frac{\text{frequency response in air}}{\text{frequency response in helium}} \quad (2.11)$$

or, in other words, $20 \log F = 20 \log (\text{frequency response in air}) - 20 \log (\text{frequency response in helium})$ where Beranek describes $20 \log F$ as a "pattern factor." The value of $20 \log F$ should very nearly equal zero at low frequencies and only deviate where cavity effects differ between the two conditions. In other words, the "pattern factor" indicates where cavity effects are distorting the frequency response curve in air. The lowest frequency for which unacceptable deviations from zero dB occur in the "pattern factor" is then the upper frequency limit for accurate calibrations in air. In helium, the upper frequency limit will be a factor of three higher.

Another reason for using helium is that since the acoustic refrigerators are normally operated with high pressure (approximately 10 to 20 atm) helium as the working fluid, it is important to ensure that the calibration curve at low pressure is not significantly altered at high pressures.

B. MICROPHONE THEORY

1. Piezoresistive microphone

The particular piezoresistive microphones used in this experiment possess a resistive four arm Wheatstone bridge circuit diffused into a silicon wafer which makes up the active area of the pressure sensing surface. The placement of the resistive elements is important to ensure that when the silicon wafer deforms under pressure, two arms of the bridge experience compressive (positive) stress while the other two experience tensile (negative) stress, as shown in Figure 2.1.

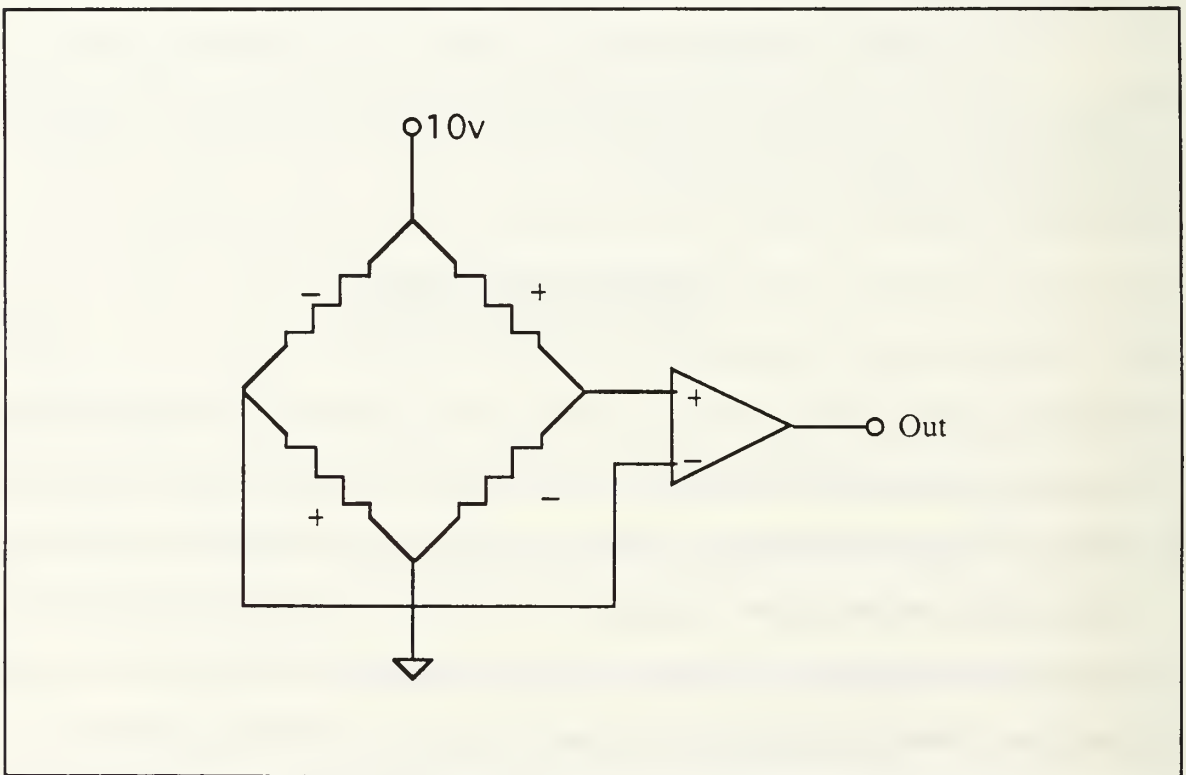


Figure 2.1 Wheatstone Bridge Diagram of the Piezoresistive Microphone.

Thus, for a given deformation, the output voltage, V , is proportional to the pressure, P , which caused the deformation. One important property of the piezoresistive pressure transducer is that since there are only resistive elements in the circuit its response is independent of frequency. Thus, a microphone of this type can have a frequency response

that is "flat" for frequencies below the fundamental resonance. This is an important property since one need only determine the sensitivity of the microphone at static pressures, a relatively simple procedure, to know its sensitivity at all frequencies below resonance. In fact, this thesis will show that this is true by determining the dynamic calibration of both piezoresistive microphones and compare them against their respective sensitivity under static pressures.

One potential problem with piezoresistive microphones is that the silicon doped resistors are very temperature dependent. The bridge configuration cancels slow temperature drifts, but the resistors may respond to temperature variations on an acoustic time scale. This depends on many things such as thermal conductivity, gas density, frequency, etc. However, it is our belief that the resistors are diffused onto the inner surface of the wafer and thus are not exposed to the temperature variations induced by the sound field.

2. Piezoelectric quartz microphone

The piezoelectric microphone is a homemade device which has, as its active sensing area, a piezoelectric quartz crystal. The quartz is a thin Y-cut disk with evaporated electrodes and a miniature FET circuit to buffer the output signal. Design and construction of the transducer are discussed in detail in reference 1. As the piezoelectric quartz wafer flexes under pressure, an electric potential is created in direct proportion to the flexure and the shear strains developed. An electrical schematic diagram of the piezoelectric quartz microphone is shown in Figure 2.2.

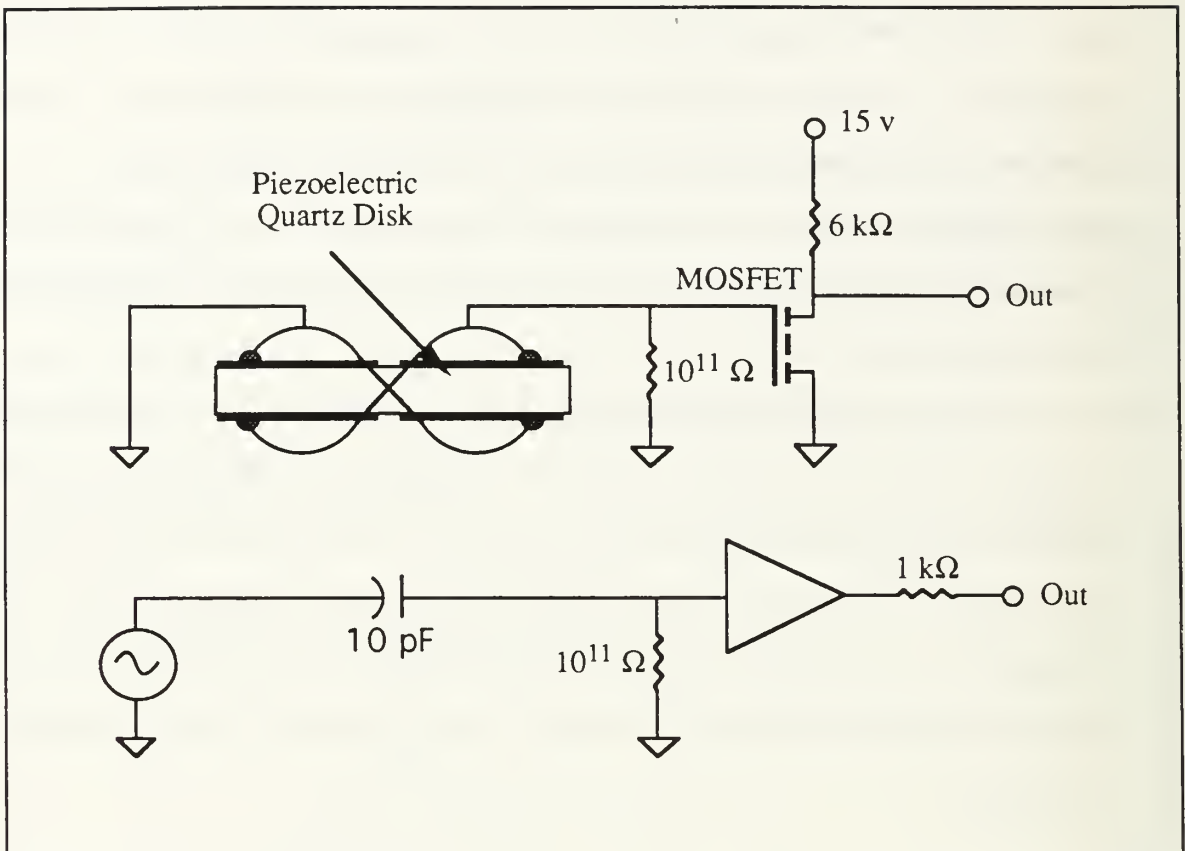


Figure 2.2 Model and Electrical Equivalent Circuit of the Piezoelectric Quartz Microphone.

The capacitance of the electrodes on the quartz crystal form low pass filter whose 3dB down point is given by

$$f_{3dB} = \frac{1}{2\pi RC} \quad (2.12)$$

where f_{3dB} is the filter 3dB down point; C is the capacitance of the quartz wafer ($\approx 10\text{pF}$); and R is the internal resistance ($\approx 10^{11}\Omega$). The result is a 3dB down point, f_{3dB} , of about 200 mHz. Since the quality of a good reference microphone is its linearity or "flatness", the piezoelectric quartz microphone is only useful well above f_{3dB} and below its fundamental resonance at about 30 kHz. An advantage of quartz is a low pyroelectric

sensitivity. The strain sensitivity of the quartz is independent of temperature variations on a fast or slow time scale.

3. Condenser microphone

A condenser microphone is basically a capacitor with one electrode being the active sensing area. As pressure deforms the active sensing area, the distance between the two plates of the capacitor is changed and thus the capacitance is changed in direct proportion to the pressure exerted on it. A bias voltage of 200 V maintains a constant charge, Q , on the capacitor. At frequencies above the low frequency roll-off, the change in voltage, ΔV , is inversely proportional to the change in capacitance, ΔC .

$$\Delta V = \frac{Q}{\Delta C} \quad (2.13)$$

and thus inversely proportion to the pressure exerted on it. As in the case of the piezoelectric microphone, the capacitance of the condenser microphone forms a high pass filter whose 3 dB down point is determined by equation 2.12. An electrical schematic of the condenser microphone is shown at Figure 2.3.

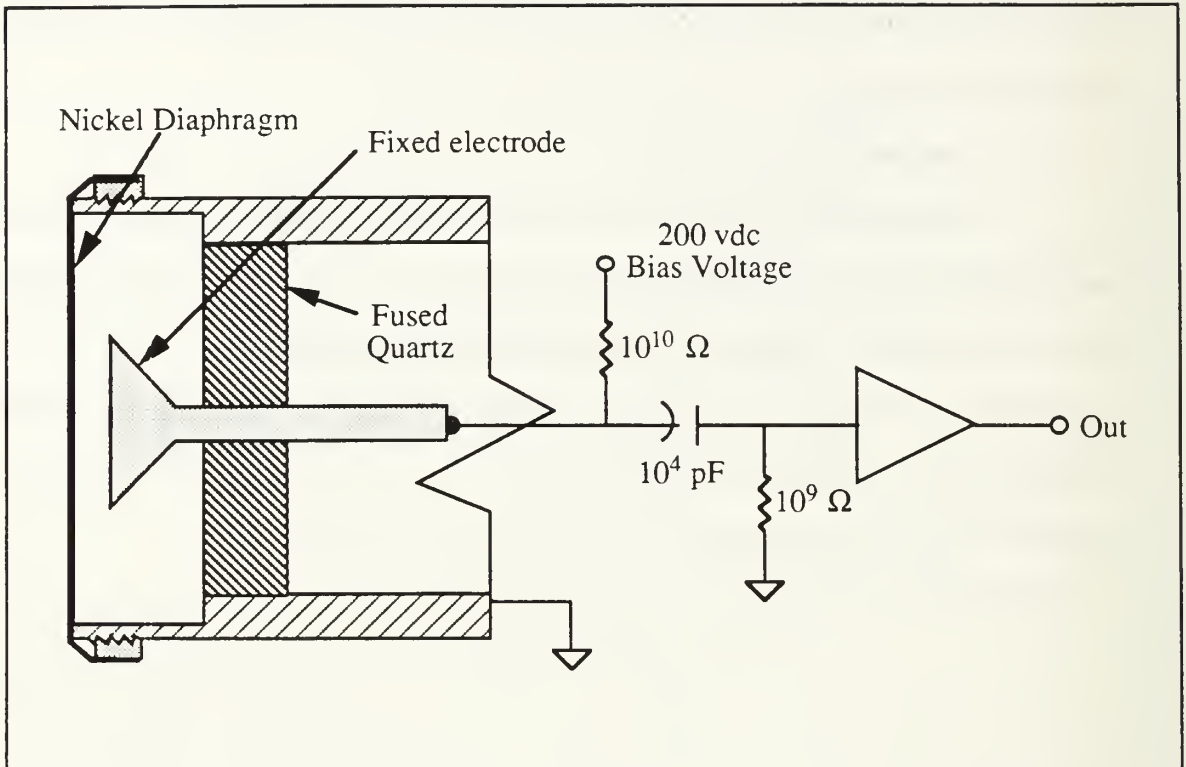


Figure 2.3 Electrical Schematic Diagram of the Condenser Microphone.

The sensitivity of the condenser microphone can be determined from either the manufacturers specifications (although these are always suspect) or by calibration using a pistonphone or similar device. A pistonphone can calibrate properly at only one test frequency which, for the particular piece of equipment used in this thesis [Ref. 6], is 251.2 Hz. Since this test frequency falls in a "flat" region of the microphone's calibration curve, then it can be assumed that the whole "flat" region shares the same sensitivity value. A pistonphone works by oscillating a piston with a known displacement in a known volume where the pressure amplitude can be calculated from the adiabatic equation of state for the gas. For ease of operation, the manufacturer supplies the known Sound Pressure Level (reference to $20 \mu\text{Pa}$) of their pistonphone for the frequency of its operation. The calculation of sensitivity of the condenser microphone, M_A , is given by

$$M_A = \frac{V}{P} \quad (2.14)$$

where V is the measured voltage output of the condenser microphone under test, and P is the known pressure, converted from the known Sound Pressure Level.

III. APPARATUS

Several pieces of apparatus are used in both the static and dynamic pressure calibrations that make up this thesis. A description of each is included in this section.

A. MICROPHONES

The primary purpose of this thesis is to calibrate a standard microphone for use in calibration of pressure transducers for acoustic power measurements. For the purposes of this thesis, four microphones are needed: the two piezoresistive microphones to be calibrated for use as the standard microphone; the condenser microphone of known calibration for comparison; and the piezoelectric quartz microphone is needed to as an interim step in the calibration process. A brief description of each is provided in this section.

1. Piezoresistive Microphone

This thesis will calibrate the two piezoresistive microphones to produce two calibrated standard microphones for acoustic power measurements. The active area of the pressure sensing surface of these microphones is made of silicon into which a four arm Wheatstone bridge has been diffused. The silicon surface has a special shape as well, which concentrates the stress at the location of the resistive elements for better sensitivity. These microphones are considered to have a linear response within the dynamic pressure range of ± 2 psig. That is, the microphone's sensitivity will remain unchanged over the dynamic pressure range.

2. Piezoresistive Microphone Housing

The piezoresistive microphone is mounted in a cylindrical housing, Figure 3.1, of machined aluminium such that its pressure sensing surface is exposed to the outside on one of the flat circular ends of the cylinder.

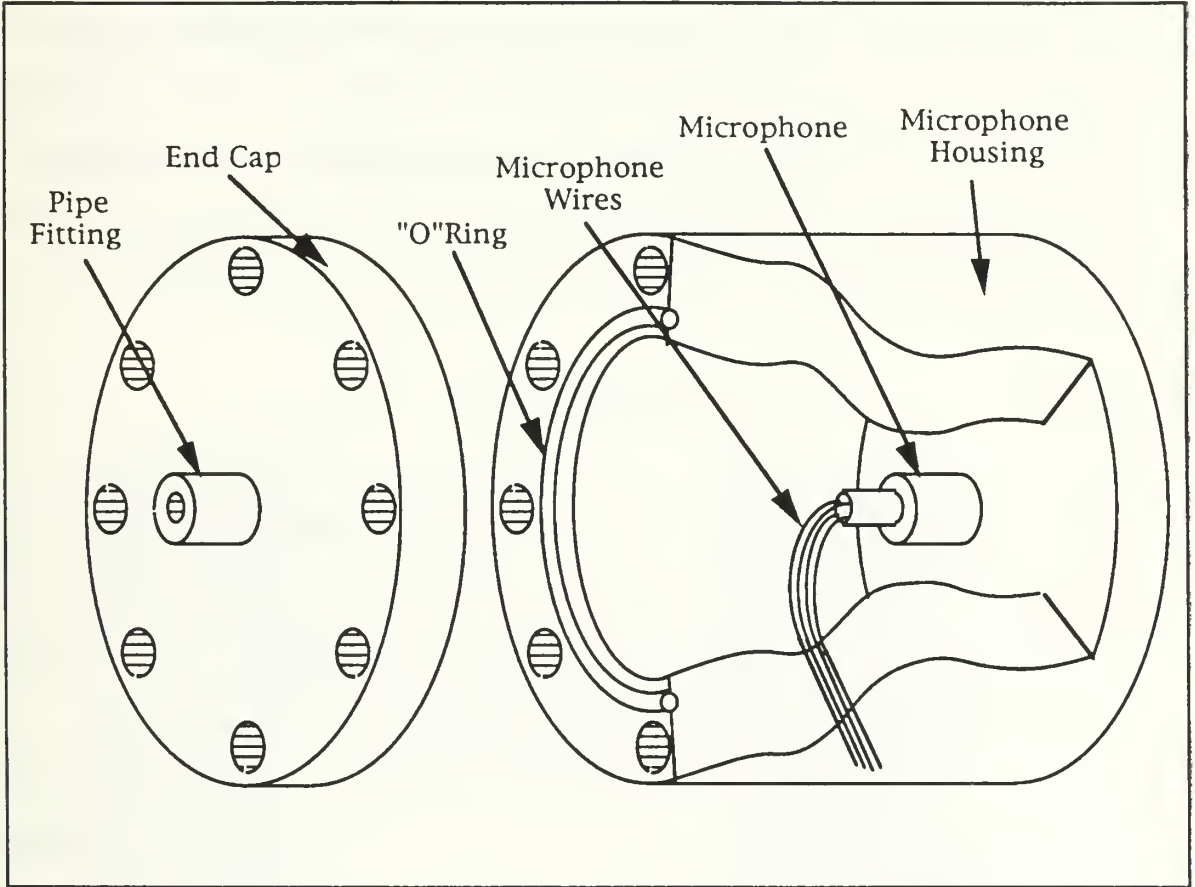


Figure 3.1 Cut-away view of the Piezoresistive Microphone Housing.

The other end of the cylinder may be sealed means of bolting on an end cap using the tapped holes around the side of the cylinder. There are other holes around the side of the cylinder which are designed so that a bolt may be passed through and the housing mounted on the dynamic pressure vessel. This allows other users of the piezoresistive microphones some flexibility for measuring acoustic power with different drivers as well as

ease of recalibration, should it become necessary. A port on the side of the housing is sealed by an epoxy plug [Ref. 7] into which four copper wires are embedded. These four wires protrude from both ends of the epoxy plug approximately 5 mm. The four wires from the microphone are each soldered onto one of the wires protruding into the cavity while the other end of these protruding wires are soldered onto wires leading to a preamplifier. Thus, the cylinder may be sealed completely and still allow electrical connections to the microphone. In order to prevent any damage to the microphone due to large pressure differentials, a capillary tube is mounted and fixed in place by epoxy [Ref. 8] into the end cap. The length, l , of the capillary tube is given by the relationship:

$$l = t \frac{P R^4 \pi}{V \eta 16} \quad (3.1)$$

where t is the desired time constant, P is the inside pressure in the housing volume, V is the inside volume of the housing, R is the radius of the capillary tube, and η is the shear viscosity. For a desired time constant of approximately 2 sec, the result was a capillary tube of .004" inside diameter and approximately 10 mm in length.

The end cap of the housing is also fitted with a pipe fitting that may be sealed or connected to pressurizing apparatus for high pressure experiments. A duplicate of the end cap (less the capillary tube) is also available to seal off, by use of 'o'rings, the microphone end of the housing for static pressure experiments.

3. Piezoelectric Quartz Microphone

The interim microphone is a piezoelectric type where the piezoelectric material used is a thin quartz disk of 1/4" diameter. It is mounted in a recessed part of the wall of the dynamic pressure vessel which is described in further detail in section B of this chapter.

It is important to note that the back volume of the quartz disk is coupled to the back volume of the driver via a tiny capillary leak.

4. Condenser Microphone

The microphone of known calibration is a condenser type microphone. This microphone must be used with a microphone power supply [Ref. 9] and a preamplifier unique to the microphone manufacturer [Ref. 10]. The manufacturer's specifications indicate that the microphone response is "flat" between 20 and 5000 Hz. To achieve this frequency response, the protective cap must be removed from the microphone and the

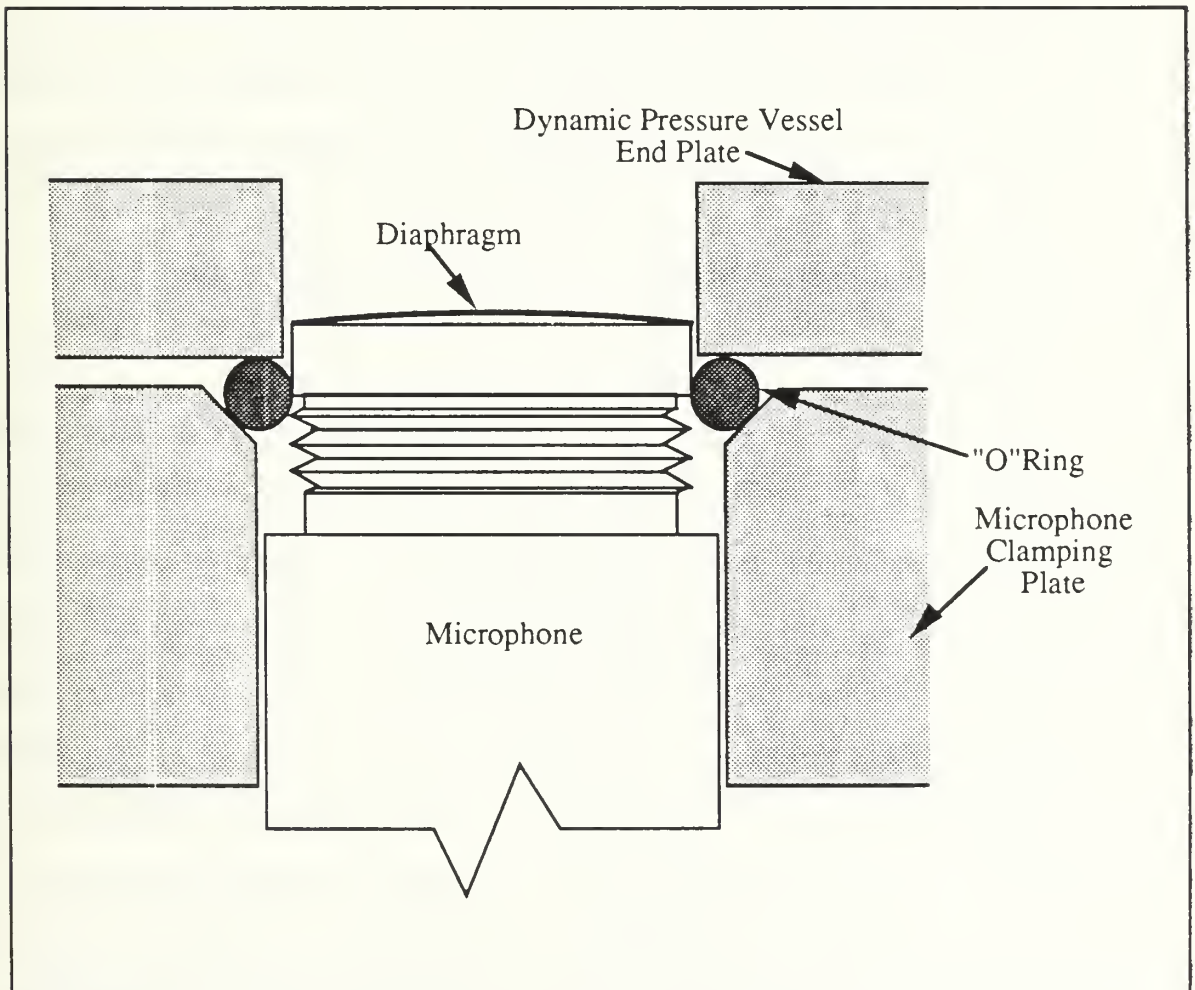


Figure 3.2 Mounting Diagram of the Condenser Microphone.

pressure sensing membrane and the sound field isolated from the back volume vent by means of an 'o'ring around the microphone housing, see Figure 3.3. The same mechanism that isolates the pressure sensing membrane also secures the microphone to the dynamic pressure vessel end plate.

A circular aluminum plate with a 0.25" hole drilled in its center and a small recess at the lip of the hole is passed over the microphone body. A snug fitting 'o'ring is also passed over the microphone body and pressed into the recess. The plate is then mounted onto the dynamic pressure vessel (using the same tapped holes that are used to mount the piezoresistive microphone housing) such that the the microphone sensing membrane passes cleanly into the 0.25" hole on the front plate. This forces the 'o'ring to be pressed against the body of the 1/4" microphone and the two plates simultaneously, effectively isolating the sound field from the back volume vent. Failure to isolate the vent will cause variations in the frequency response at low frequencies.

B . DYNAMIC PRESSURE VESSEL

The dynamic pressure vessel has a cylindrically shaped cavity and is constructed of machined aluminium, Figure 3.4, for use in the dynamic pressure experiments. At one end of the cavity is mounted the hemispherical driver [Ref. 11]. This driver is adhered to the cylinder walls using a silicon sealant [Ref. 12] and it's back volume is enclosed with by a cylindrical aluminum end cap. On the other end of the cavity, a circular end plate is mounted in which is drilled a hole of diameter large enough to fit the 1/4" condenser or piezoresistive microphone. This plate also has tapped holes for mounting either the piezoresistive microphone housing or the 1/4" condenser microphone holding plate. At approximately 90° apart on the outside wall of the cylinder are mounted two valves (not shown in Fig 3.4). The output valve is simply ported to the outside, while the input valve is connected to the driver back volume as well as the piezoresistive microphone housing

back volume through copper tubing. Recessed into the inside wall of the cavity is located the piezoelectric quartz microphone (not shown in Fig 3.4). The back volume of the quartz microphone is vented to the driver back volume. Thus, by connecting all the copper tubing from the back volumes to the input valve, the apparatus can be pressurized without creating large pressure differentials across the microphone diaphragms or the driver diaphragm.

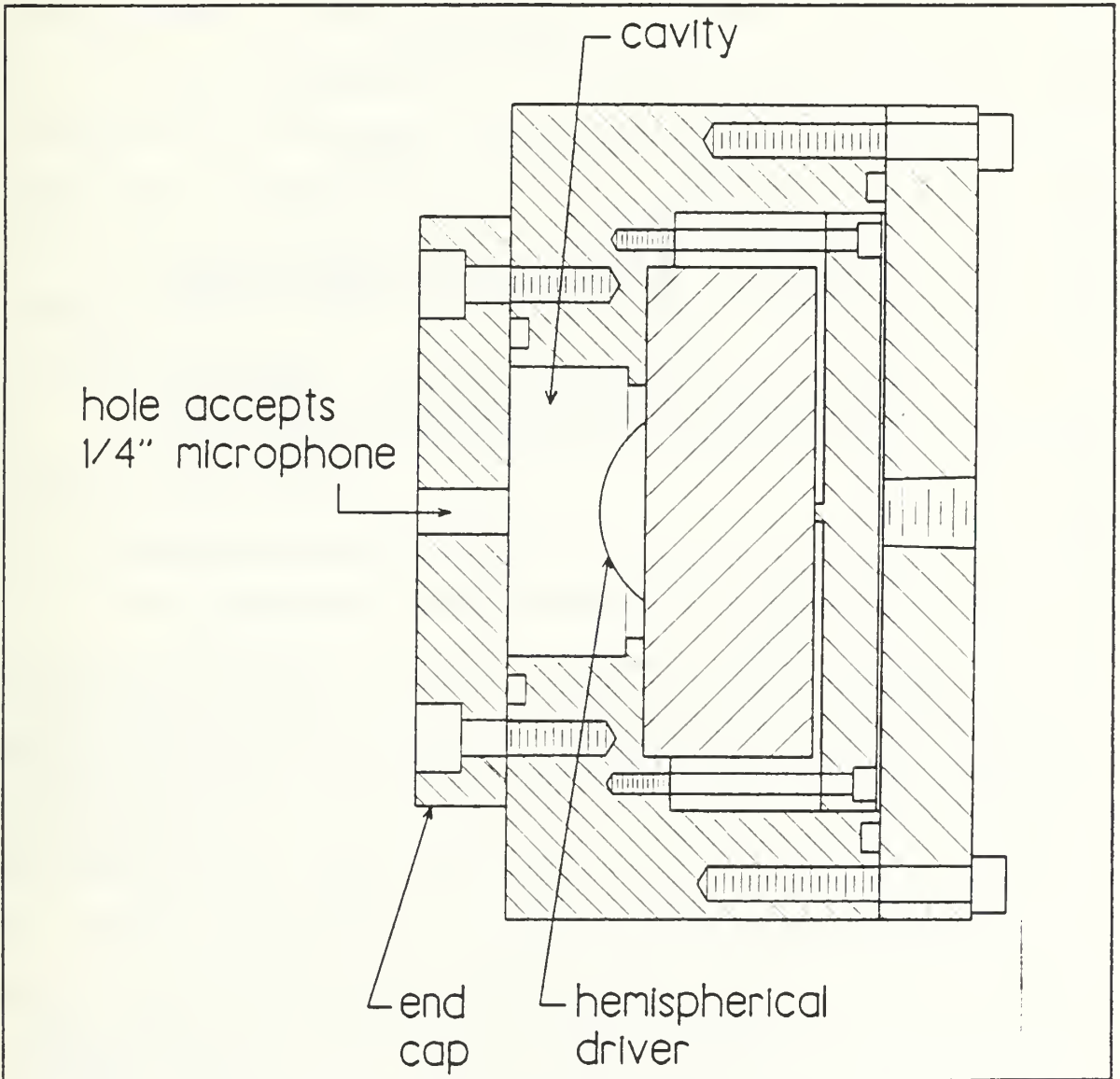


Figure 3.3 Dynamic Pressure Vessel.

C. MEASUREMENT EQUIPMENT

1. Static Calibration Apparatus

During the static calibration experiment, the apparatus was set up as shown in Figure 3.4.

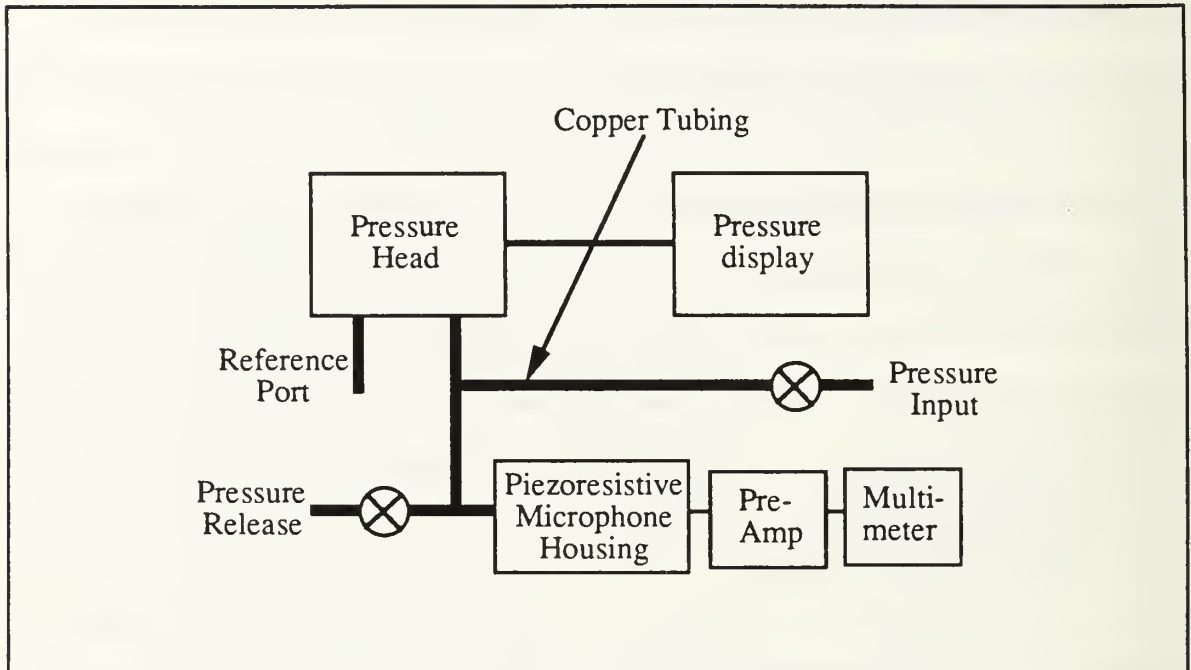


Figure 3.4 Static Calibration Apparatus.

The pressure sensing surface of the piezoresistive microphone is isolated from the room pressure by mounting an aluminium cap to the microphone end of the housing and sealing the joint with an 'o'ring. The back volume is left open to the room through the capillary tube. The cap is connected through copper tubing to a pressure sensing head [Ref. 13] as well as a valve through which pressure can be input into the apparatus. The pressure sensing head works by sensing the differential pressure between the sensing port which is connected to our apparatus and the reference port which is left open to the ambient room pressure. A metal disk flexes in response to the pressure difference and the amount

of flexure is measured by a capacitance bridge where the disk forms half of two capacitors. This signal is converted to a suitable pressure signal and is displayed digitally. It is important to note that the pressure sensing head was calibrated by the manufacturer just prior to these measurements and I am therefore confident of the results. I have included the results of the calibration as Figure 3.5. Since the maximum static pressure I used was about 150 mmHg, I can expect an worst case error in the pressure reading of 0.02%.

The static calibration apparatus operates as follows: The pressure head interprets the pressure relative to the room pressure and converts the information to an electronic signal which is displayed on a pressure display unit [Ref. 14]. The electrical response from the piezoresistive microphone is amplified by a home-made preamplifier and displayed on a digital multimeter [Ref. 15]. The schematic diagram of the pre-amplifier is included in Appendix A.

A simple syringe is used to increase or decrease the pressure in the apparatus relative to ambient pressure.

2. Dynamic Calibration Apparatus

During the dynamic calibration experiment, the apparatus was set up as shown in Figure 3.6. The design of the dynamic pressure vessel makes it easy to exchange the piezoresistive microphone for the 1/4" condenser microphone and thus make an accurate comparison their frequency responses under the same conditions using the piezoelectric quartz microphone as an intermediate reference.

a. Piezoresistive Microphone Installed on Apparatus

The piezoresistive microphone housing is mounted on the dynamic pressure vessel. The pressure sensing surface of the piezoresistive microphone is isolated from the outside by an 'o'ring but exposed to the sound field inside cavity of the dynamic pressure



CALIBRATION RECORD SHEET

The following data was measured on the MKS Baratron Head identified by Type and Serial Number. Calibration is performed using an MKS Transfer Standard that has been calibrated with a CEC Air Dead-Weight Tester which is traceable to the National Institute of Standards and Technology.

<u>CALIBRATION DATA</u>			
Pressure Std. mmHg	Computed Linear DC. Output	Incoming Error (\pm mV)	Error (\pm mV)
.00	.0000	+263mV	+/-0MV
100.82	1.0082		+0.2
201.64	2.0164		+0.2
302.46	3.0246		-0.1
403.28	4.0328		-0.9
504.10	5.0410		-2.5
604.91	6.0491		-4.2
705.73	7.0573		-6.0
801.38	8.0138		-7.1
904.79	9.0479		-5.9
1008.19	10.0819		+1.1

Head Type 370HD-1000 Data by TT
 Ser. No. 22573-1 Chk. by _____
 Indicator Type 390HA-01000 Date 03/24/92
 Ser. No. 36335-1A Sys. Chk. 9.940V

NOTES:

1. Temperature regulated units must be operated on regulated heat approximately 4 hours before check or resetting calibration.
2. Bakeable Heads are calibrated at 25 C. and Temp. Comp. pot set at 500.
3. MKS DIGITAL READOUTS READ DIRECTLY IN PRESSURE.

Figure 3.5 Pressure Head Calibration Chart.

vessel. For low or room pressure experiments the back volume of the piezoresistive microphone can be left open to the room through the capillary tube and the back volume of the driver can also be left open to the room through the pipe fitting in the back plate of the dynamic pressure vessel. For high pressure experiments where the cavity and back volumes are filled with helium, copper tubing is used such that the entire apparatus can be

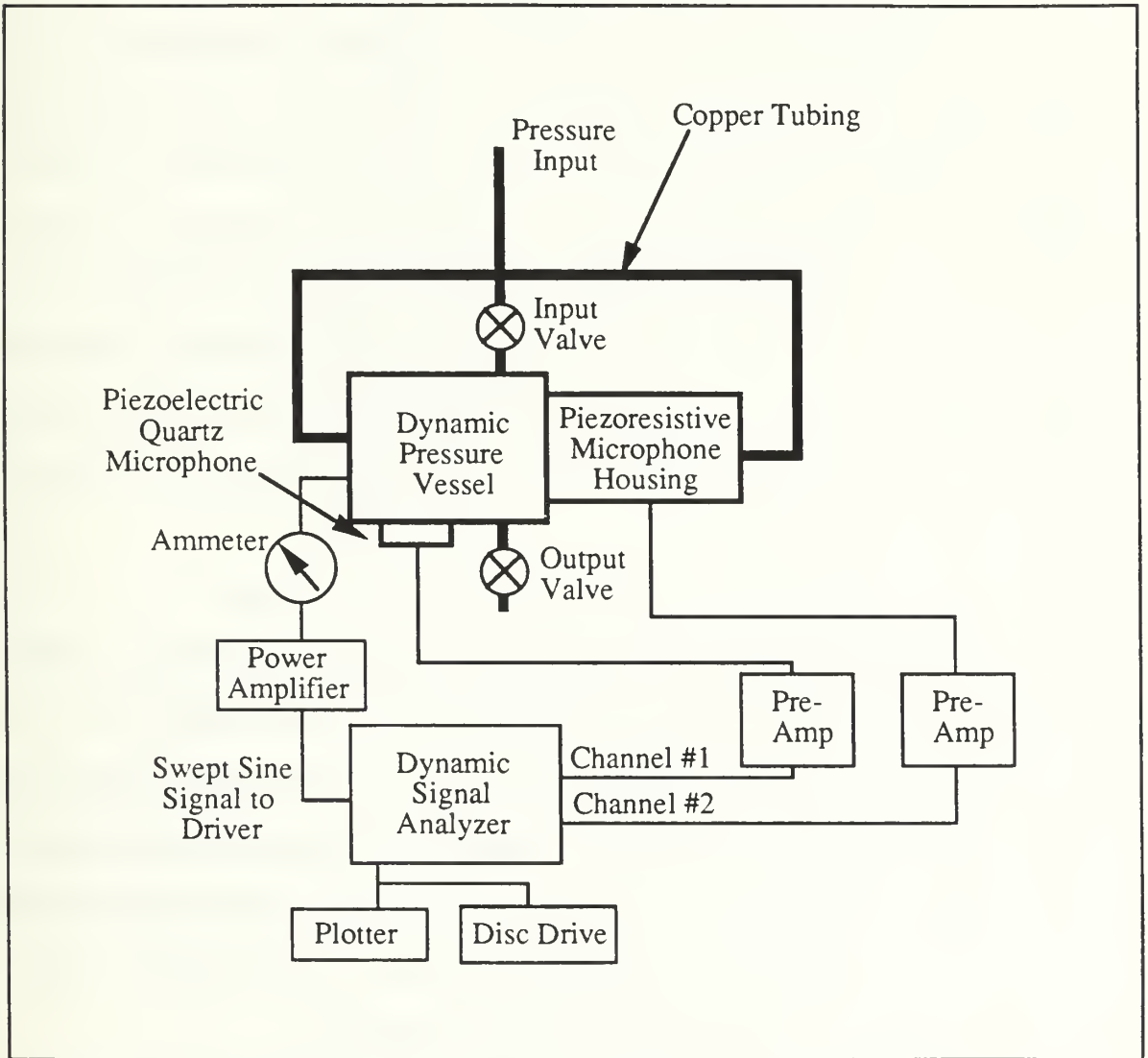


Figure 3.6 Dynamic Calibration Apparatus.

isolated from the room. This is achieved by connecting the copper tubing from the pipe fitting on the end cap of the piezoresistive microphone housing to the pipe fitting on the back of the dynamic pressure vessel back plate and to the input valve to the cavity. There is also a short piece of tubing for filling the apparatus from the pressure source.

The hemispherical driver is driven by a signal generated from a two channel dynamic signal analyzer [Ref. 16] and amplified through a power amplifier [Ref. 17]. The current from the power amplifier is monitored by a multimeter [Ref. 18] to reduce the risk of overdriving the driver. The electrical response from the piezoresistive microphone is amplified by the same preamplifier that was used in the static experiment and recorded on channel 2 of the dynamic signal analyzer. The electrical response from the piezoelectric microphone that is built into the dynamic pressure vessel is amplified by a preamplifier [Ref. 19] then recorded on the reference input, channel 1, of the dynamic signal analyzer. Also connected to the dynamic signal analyzer is a plotter [Ref. 20] and a 3.5" floppy disk drive [Ref. 21] for data storage.

b. Condenser Microphone Installed on Apparatus

With the 1/4" condenser microphone installed instead of the piezoresistive microphone, the electrical response is amplified by an preamplifier unique to the microphone manufacturer and recorded on channel 2 of the dynamic signal analyzer. The dynamic signal analyzer is a useful piece of equipment for these experiments in that it not only can carry out the basic frequency response functions, it can store and mathematically manipulate the data in order to produce useful results.

3. Condenser Microphone Calibration Apparatus

In order to confirm the calibration of the reference condenser microphone a device which produces a known and accurate Sound Pressure Level is used, Figure 3.7.

The device is a portable, battery driven calibrator called a pistonphone. With the 1/4" condenser microphone properly seated in the open end, the pistonphone is switched on and produces a nominal sound pressure field of 124 dB re 20 μ Pa at 251.2 Hz. The

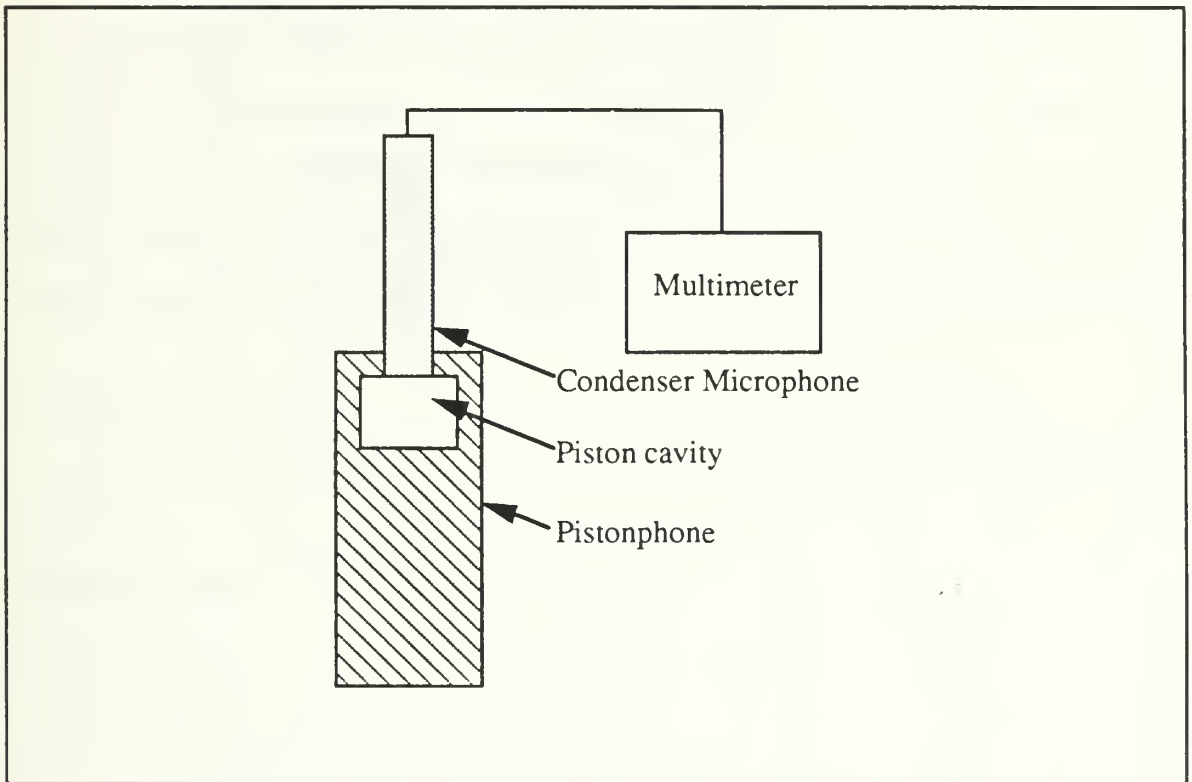


Figure 3.7 Condenser Microphone Calibration Apparatus

electrical response of the microphone is measured and the sensitivity is calculated as described in equation 2.14. It is important to note that the pistonphone was calibrated by the manufacturer just prior to these measurements and I am therefore confident of the results. I have included the results of the calibration as Figure 3.8.



Acoustics
Garrett FH/Cs
NPS Foundation

Calibration Chart

Pistonphone Type 4228

Corrections:

If the pistonphone is used under conditions different to the stated Reference Conditions, the sound pressure level produced is found from the following equation.

$$\text{Actual SPL} = \text{Stated SPL} + \Delta L_p + \Delta L_v$$

Serial No: 1681325
 Sound Pressure Level: 124.08 re 20 μ Pa

The stated level is traceable to NIST and valid at the following Reference Conditions:

- Ambient Static Pressure: 1013 hPa
- Ambient Temperature: 20 °C
- Relative Humidity: 65% RH
- Effective Load Volume: 1333 mm³

The uncertainty of the calibration value is less than 0.09 dB (99% confidence level)

Nominal Frequency: 250 Hz

Exact Frequency: 10⁻⁴ Hz (ISO 266) or 251.2 Hz \pm 0.1%

The pistonphone was calibrated at the following ambient conditions.

Pressure: 1000 hPa Temperature: 25 °C Humidity: 50 % RH

25-8-92 Date CV Calibrated
4-9-92 Date OL Approved

Pistonphone Type 4228 complies with IEC 942 (1988) Class 1L and ANSI S1.40-1984

The correction for the ambient pressure, ΔL_p , can be read directly from Correction Barometer UZ0004

The correction for the load volume, ΔL_v , can be read from the table below

Size	Pistonphone Adaptor	Microphone Type	Load Volume Correction, ΔL_v (dB)		
			With Protection Grid	Without Protection Grid	With Adaptor Ring UA0825
1"	Nona	4131/32	0.05		+0.25
		4144/45	+0.05		+0.25
		4160 4179	+0.43 0.05	+0.28	
1/2"	DP-0776	4129/30	-0.02		
		4133/34	0.00		+0.08
		4147	0.00		+0.08
		4148	-0.04		
		4149	0.00		
		4155	0.03		
1/4"	DP-0775	4165/66	0.03		
		4176	0.02	+0.08	
		4180 4181	0.00		
1/8"	DP-0774	4183	-0.02		
1/16"	DP-0774	4138	0.00		

10-200427

For further information, or if the pistonphone is used as a calibrator complying with IEC 942 (1988) Class 0L, consult the instruction manual

Figure 3.8 Pistonphone Calibration Chart.

IV. THE STATIC PRESSURE TEST

We expect the frequency response of piezoresistive microphones to be frequency independent ("flat") from static pressure up to the region approaching the fundamental resonance. This experiment will determine the static pressure sensitivity and compare it to the manufacturer's sensitivity specification for the two microphones. The two piezoresistive microphones calibrated during this experiment will be referred to as piezoresistive microphones #1 [Ref. 23] and piezoresistive microphones #2 [Ref. 24].

A. EXPERIMENT

The piezoresistive microphone was mounted in its housing with the pressure sensing diaphragm exposed to the source of static pressure through an arrangement of copper tubing, see Figure 3.4. The source of static pressure used was a small syringe filled with air which would be slowly injected into the tubing. The microphone electrical output signal was amplified then displayed on a digital multimeter. A pressure sensing head was, at the same time, exposed to the pressure and its output signal was displayed on a digital pressure readout device. The accuracy of the instrument, as given by the manufacturer is $\pm 0.02\%$.

The experiment was conducted by increasing the pressure in the copper tubing until the pressure readout indicated the maximum static pressure at which the microphone sensitivity would remain linear. Closing off the input valve locked the pressure inside the apparatus. By bleeding off a small amount of pressure at a time, several readings for static pressure and DC voltage were recorded. The procedure was repeated except this time air was extracted out of the copper tubing creating a partial vacuum and small amounts of pressure was let in.

B. RESULTS

The results were plotted here as voltage vs. pressure. A linear regression of the data points for each microphone and the slope error was calculated. The gain on the preamplifier was 100.15 or 40.013 dB.

It must be noted that the manufacturers specifications for these particular resistive bridge microphones claim that their response is linear only between a ± 2 psi pressure range. Therefore, when calculating the slope and the slope error in Figure 4.1, only data points which fall in that range were used.

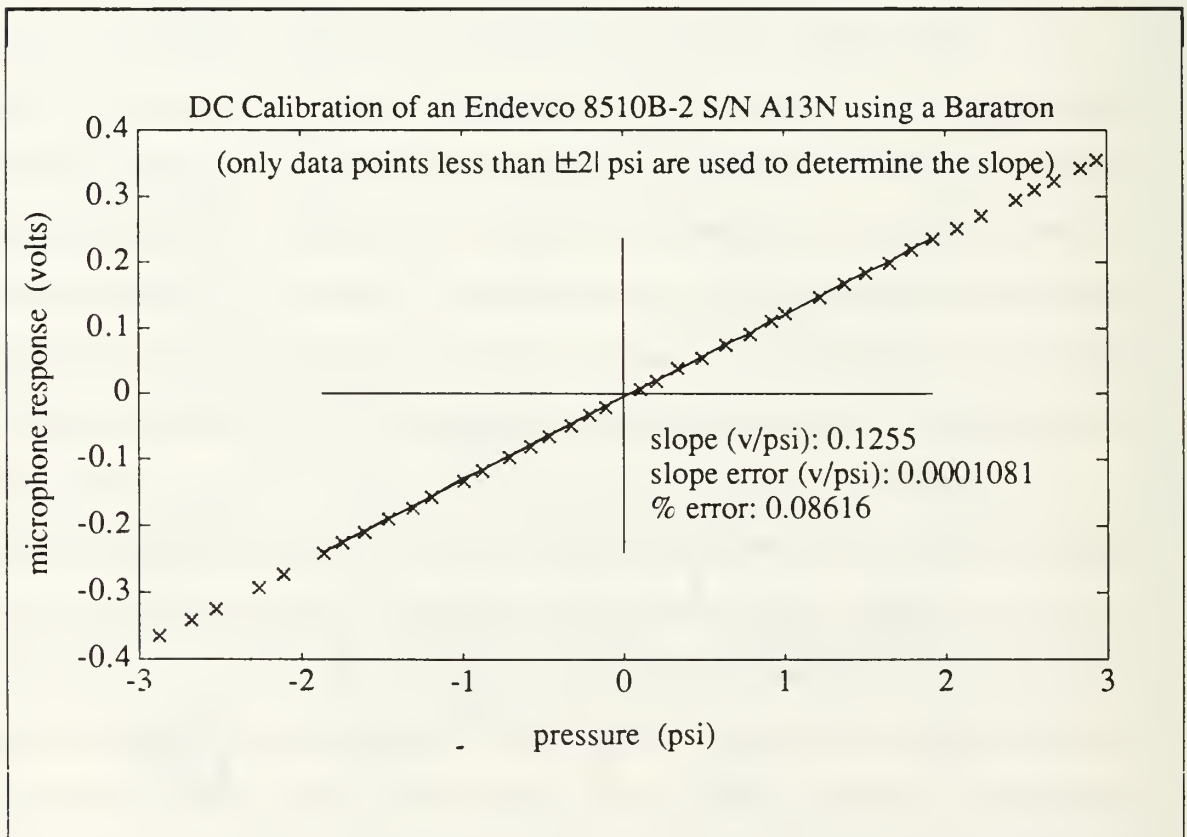


Figure 4.1 Static Calibration of Piezoresistive Microphone #1 for Data Points below ± 2 psi.

As well, I have plotted and calculated the microphone sensitivity and uncertainty for all data points below ± 1 psi in Figure 4.2 and below ± 0.5 psi in Figure 4.3.

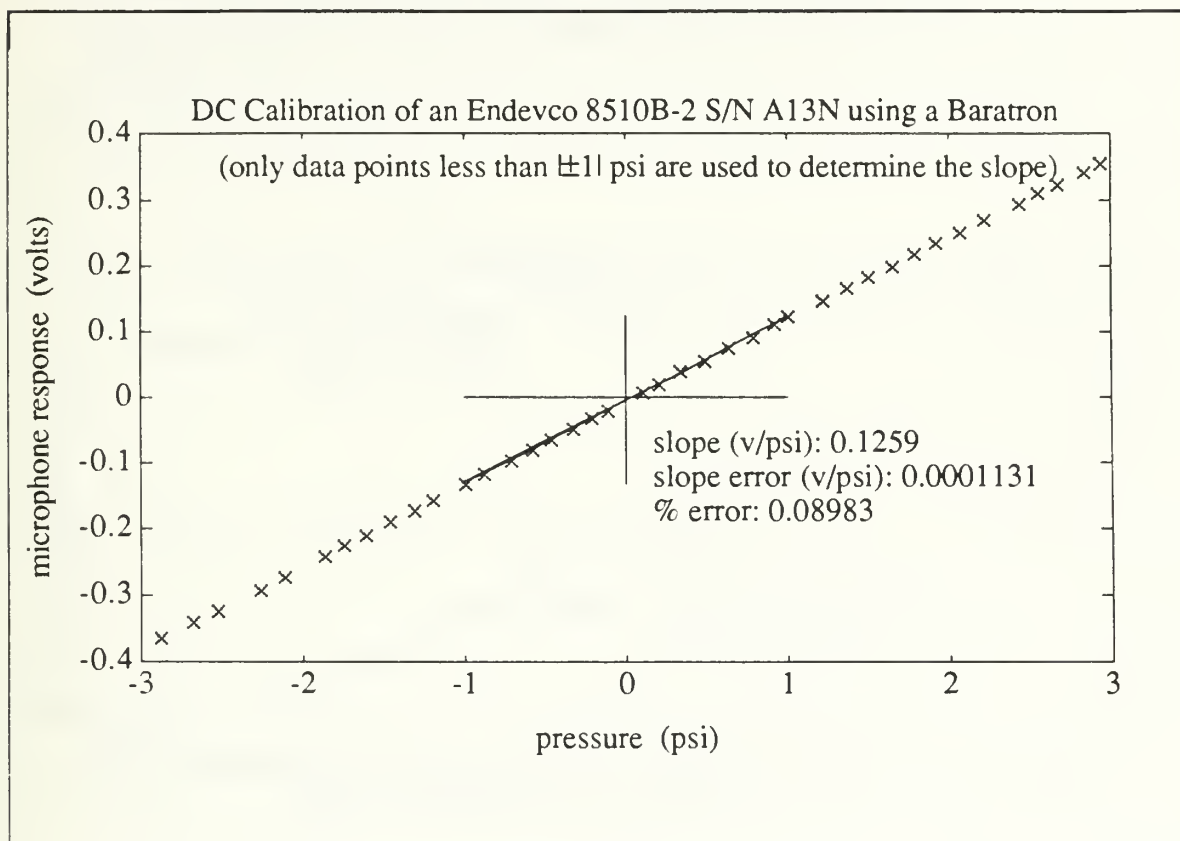


Figure 4.2 Static Calibration of Piezoresistive Microphone #1 for Data Points below ± 1 psi.

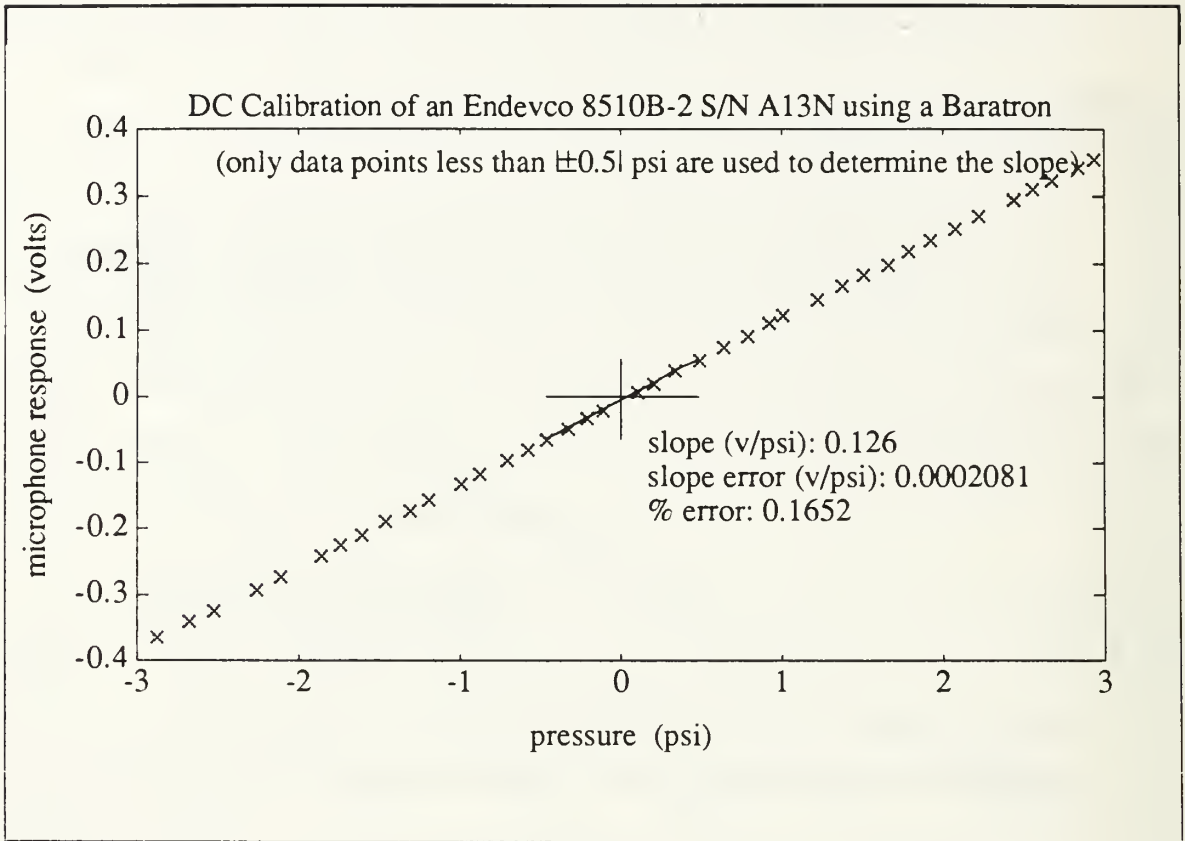


Figure 4.3 Static Calibration of Piezoresistive Microphone #1 for Data Points below ± 0.5 psi.

As I take a progressively smaller range of data points for the calculation, the slope of the line and thus the calculated sensitivity increases. This would indicate a systematic error somewhere in the data. I expect the linear regression of the data points of the smaller pressure range would be the most accurate since the microphone is more linear here. However, since below 0.5 psi there are few data points to use, I will chose the information from the data collected below 1 psi i Figure4.2 for further discussion in this thesis.

The plot for the static calibration of piezoresistive microphone #1 are linear as expected. The value of the slope of this plot determines the constant of proportionality between the pressure and the voltage output of the microphone. Factoring out the gain of the preamplifier results in a microphone sensitivity of 125.9 mV/psi with a slope error of less than 0.1%. The manufacturer's specifications quote a sensitivity of 125.8 mV/psi.

The discrepancy between this value and my experimentally determined value is less than 0.1%.

The same analysis was applied to the microphone #2 and the information from the data collected below ± 1 psi is plotted in Figure 4.2 for further discussion in this thesis.

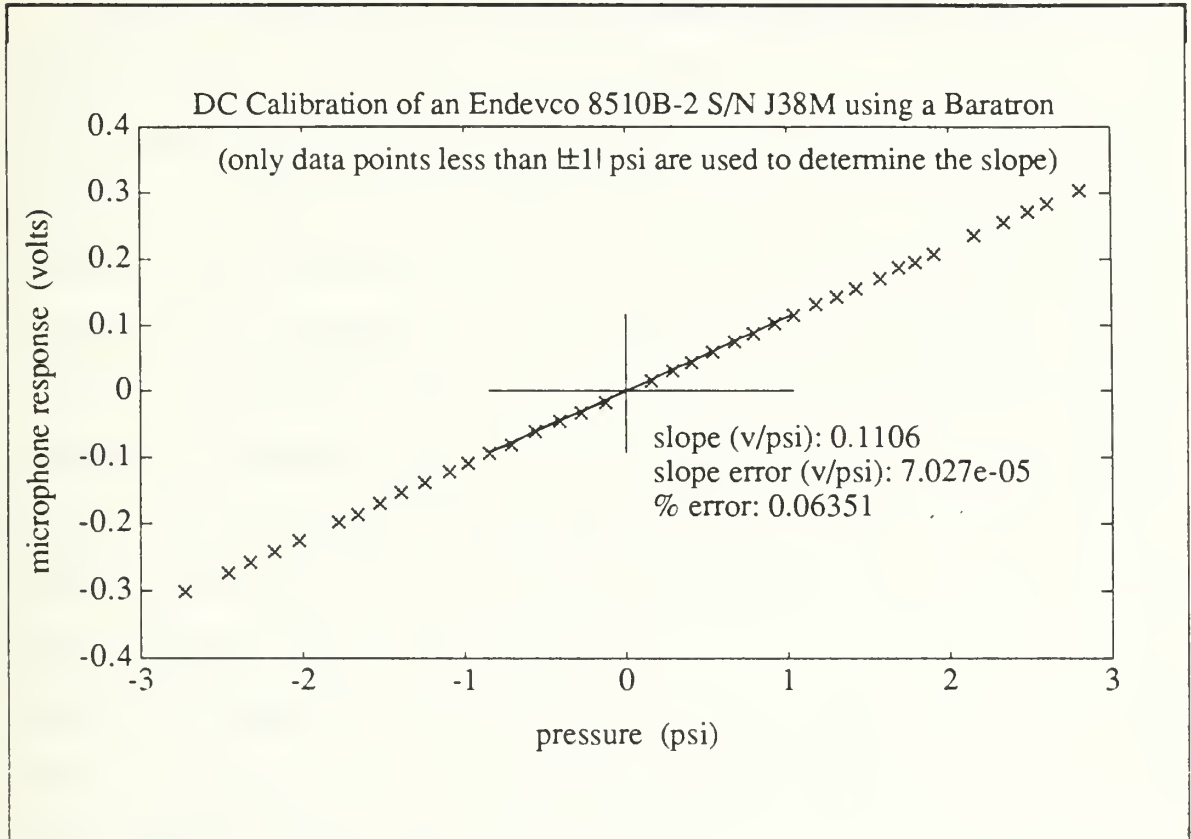


Figure 4.4 Static Calibration of Piezoresistive Microphone #2 for Data Points below ± 1 psi.

The plot for the static calibration of piezoresistive microphone #2 are linear as expected. The value of the slope of this plot determines the constant of proportionality between the pressure and the voltage output of the microphone. Factoring out the gain of the preamplifier results in a microphone sensitivity of 110.6 mV/psi with a slope error of less than 0.1%. The manufacturer's specifications quote a sensitivity of 111.1 mV/psi. The discrepancy between this value and my experimentally determined value is 0.4%.

With this information we can speculate that the dynamic sensitivity for frequencies below the fundamental resonance are the same as the value for static sensitivity. The next step is to determine the dynamic frequency response for each microphone to ensure that the value for the static sensitivity is actually valid to within 1% error at the frequencies of concern for acoustical power measurements.

V. THE DYNAMIC PRESSURE TEST

A. PIEZORESISTIVE MICROPHONE FREQUENCY RESPONSE

The set up of this experiment is described in Chapter III of this thesis. The experiment began by mounting a piezoresistive microphone housing to the dynamic pressure vessel and applying a swept sine signal from the dynamic signal analyzer through the power amplifier to the driver. The two piezoresistive microphones calibrated during this experiment will be referred to as piezoresistive microphones #1 and piezoresistive microphones #2. A frequency range of 1 to 1000 Hz was used mostly throughout the experiment since the range of most interest for the thermoacoustic refrigerator is about half the upper limit of 1000 Hz. However, the experiment did start the frequency range as low as 0.1 Hz or end the frequency range as high as 3000 Hz on at least one occasion in order to satisfy my concern that the frequency response curve was held no surprises outside the range of interest. Also, we were concerned about any very low frequency response anomalies that might invalidate the assumption that the static response and the low frequency response are the same. A potential source for such an anomaly could be very slow temperature variations caused by changes in the current exciting the resistors in the piezoresistive microphone. The dynamic calibration experiments involving the piezoresistive microphone were conducted under these conditions in the following media: low pressure air, low pressure helium, and high pressure helium.

1. Fluid Medium: Low Pressure Air

The cavity was sealed off completely with air at atmospheric pressure, however, the back volume of the driver and the piezoresistive microphone are left open to the room pressure. The frequency response output of the piezoresistive microphone was recorded by the dynamic signal analyzer in decibels, referenced to the frequency response output of the piezoelectric quartz microphone.

2. Fluid Medium: Low Pressure Helium

The cavity and backsides of the driver and the piezoresistive microphone housing are connected via copper tubing and isolated from the ambient air. Helium was very slowly pumped into the apparatus to approximately 10 atms and then the pressure was bled off. Care was taken during this process to ensure that the microphones would pressurize equally on both sides in order that they not be damaged. This process was repeated three times in order to purge the apparatus of air, leaving only dry helium inside the cavity and the back volumes of the driver and the piezoresistive microphone.

With the helium pressurized to 15 psia, the frequency response output of the piezoresistive microphone was recorded by the dynamic signal analyzer in decibels, referenced to the frequency response output of the piezoelectric quartz microphone.

3. Fluid Medium: High Pressure Helium

With the apparatus left the same as it was for low pressure helium, the pressure of the helium was then increased to 132.5 psia and the frequency response output of the piezoresistive microphone was recorded by the dynamic signal analyzer in decibels, referenced to the frequency response output of the piezoelectric quartz microphone.

B. CONDENSER MICROPHONE FREQUENCY RESPONSE

The set up of this experiment is described in the Apparatus chapter of this thesis. Ensuring that all pressure was carefully removed from the apparatus, the piezoresistive microphone housing was removed and a 1/4" condenser microphone was mounted into the front plate of the dynamic pressure vessel as described in Chapter III. The dynamic calibration experiments involving the condenser microphone were conducted under these conditions in the following media: low pressure air and low pressure helium.

1. Fluid Medium: Low Pressure Air

The cavity of the dynamic pressure vessel was sealed off completely with air at atmospheric pressure and the backsides of the driver are left open to the room air. Since

the 1/4" capacitive microphone has no external sealed housing similar to the piezoresistive microphone housing, it can only be left exposed to the room pressure. The frequency response output of the condenser microphone was recorded by the dynamic signal analyzer in decibels, referenced to the frequency response output of the piezoelectric quartz microphone.

2. Fluid Medium: Low Pressure Helium

To inject helium into the apparatus with the condenser microphone attached, the back volume of the driver and the capacitive microphone were left open to the room air and the input and output valves of the dynamic pressure vessel were also open. Helium was then allowed to very slowly blow through the cavity. After approximately five minutes the input valve is closed and immediately after, the output valve is closed. This sequence of actions should prevent any over pressuring of the cavity as well as preventing air from re-entering the cavity through the output port. Although it is expected that there may be significant amounts of air mixed with helium remaining in the cavity, the concentration of helium should still be high enough to cause any frequency dependent cavity effects to shift to a higher frequency, out of our range of interest. The frequency response output of the condenser microphone was recorded by the dynamic signal analyzer in decibels, referenced to the frequency response output of the piezoelectric quartz microphone.

C. RESULTS

1. Piezoresistive Microphone Frequency Response

The results of the dynamic calibration experiments involving the piezoresistive microphone are the frequency responses of this microphone measured with respect to the piezoelectric quartz microphone at frequencies from 1 to 1000 Hz in low pressure air, low pressure helium, and high pressure helium.

a. *Low Pressure Air*

In low pressure air, the response curve is shown at Figure 5.1 for the piezoresistive microphone #1 and Figure 5.2 for the piezoresistive microphone #2.

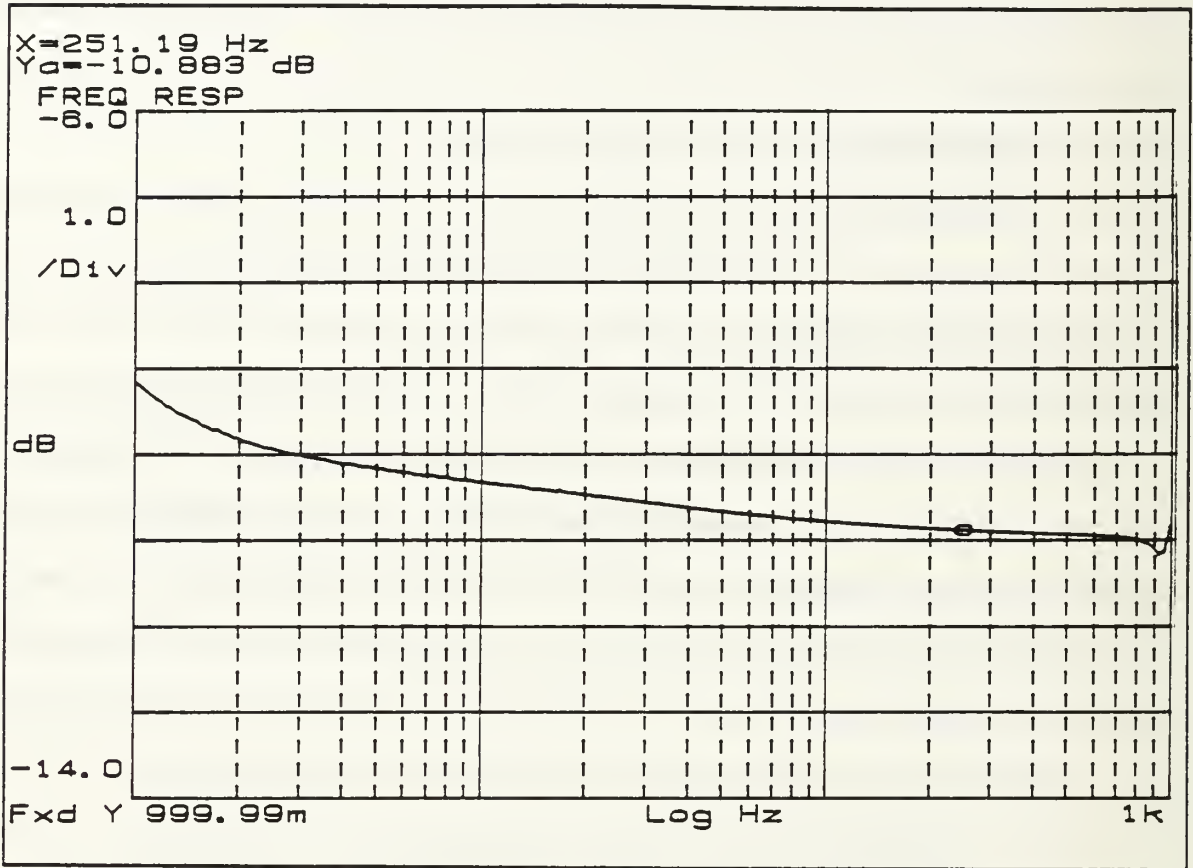


Figure 5.1 Frequency response of the piezoresistive microphone #1 with respect to the frequency response of the piezoelectric quartz microphone in low pressure air.

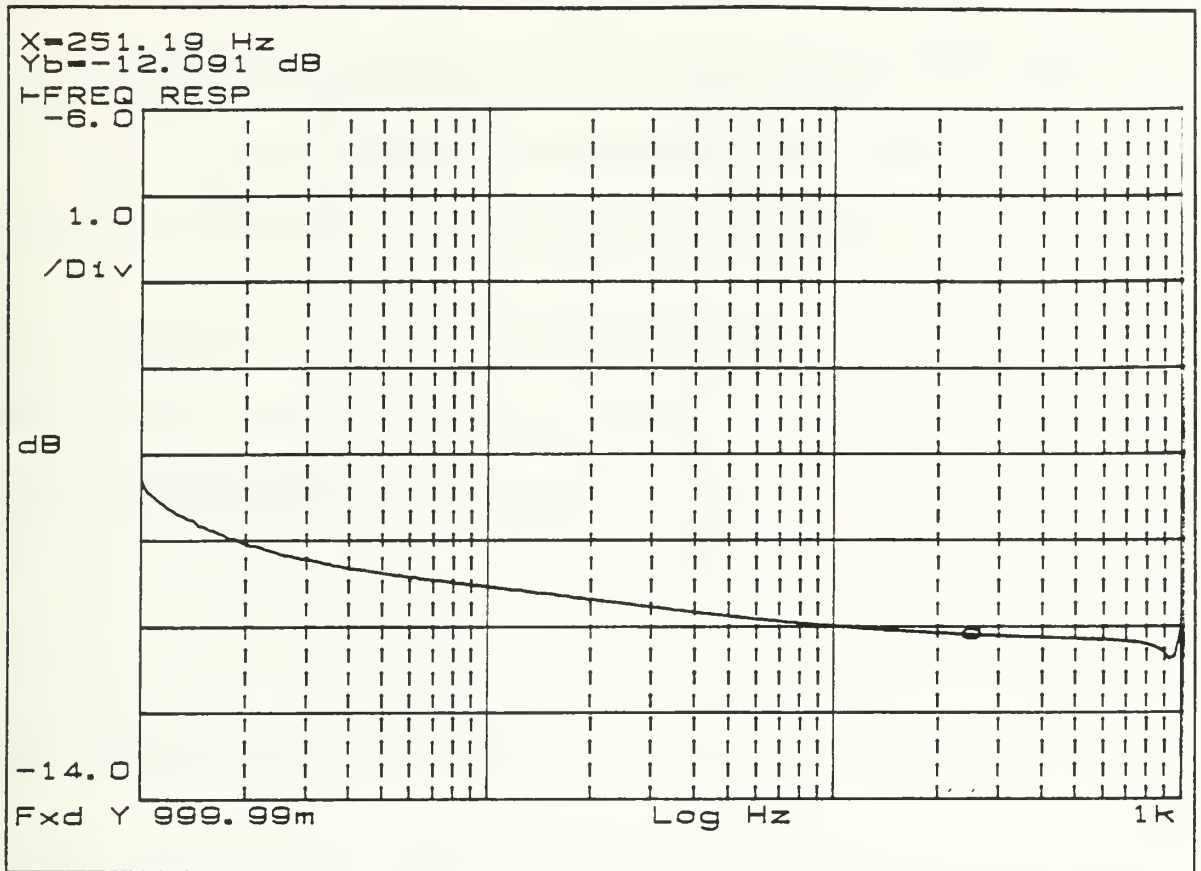


Figure 5.2 Frequency response of the piezoresistive microphone #2 with respect to the frequency response of the piezoelectric quartz microphone in low pressure air.

The reader will note that the curves show a cavity resonance occurring at approximately 900 Hz in both cases.

b. Low Pressure Helium

In low pressure helium, the response curve is shown at Figure 5.3 for the piezoresistive microphone #1 and Figure 5.4 for the piezoresistive microphone #2.

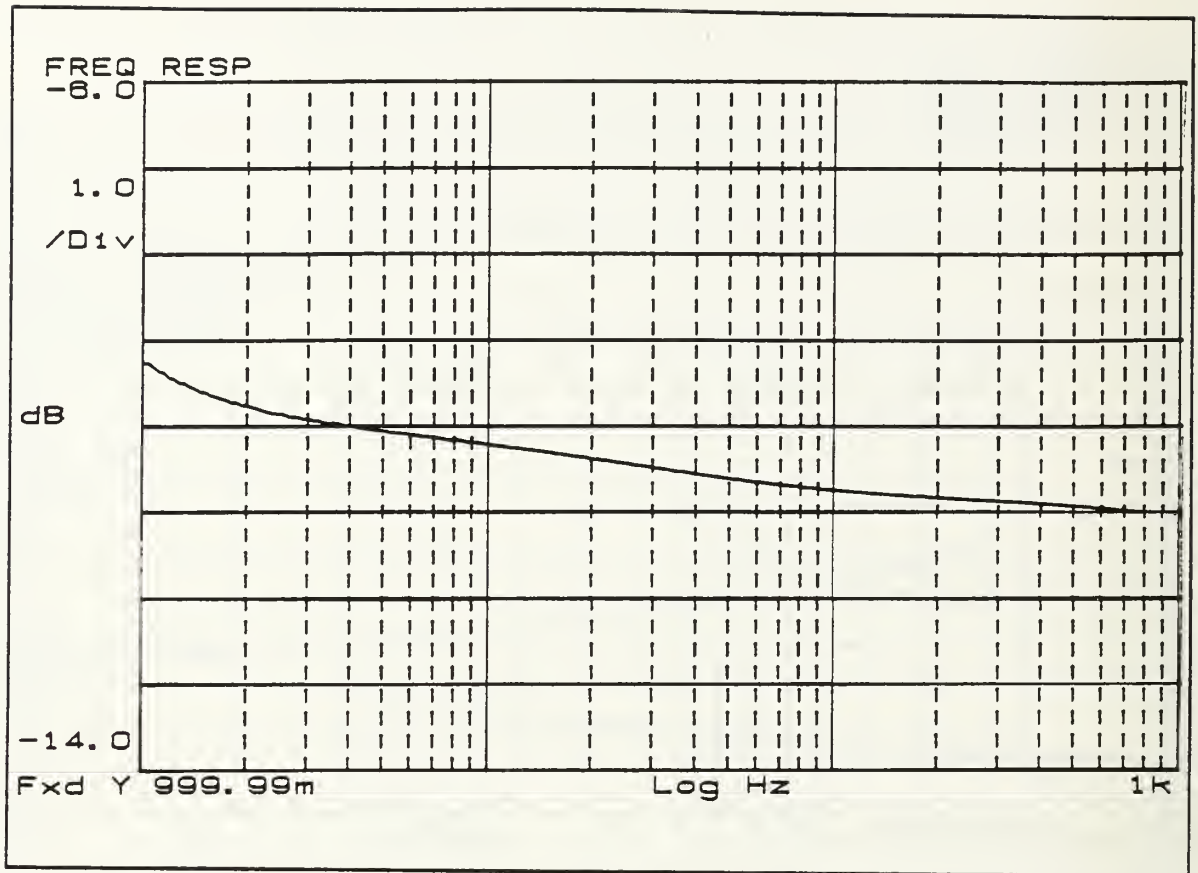


Figure 5.3 Frequency response of the piezoresistive microphone #1 with respect to the frequency response of the piezoelectric quartz microphone in low pressure helium.

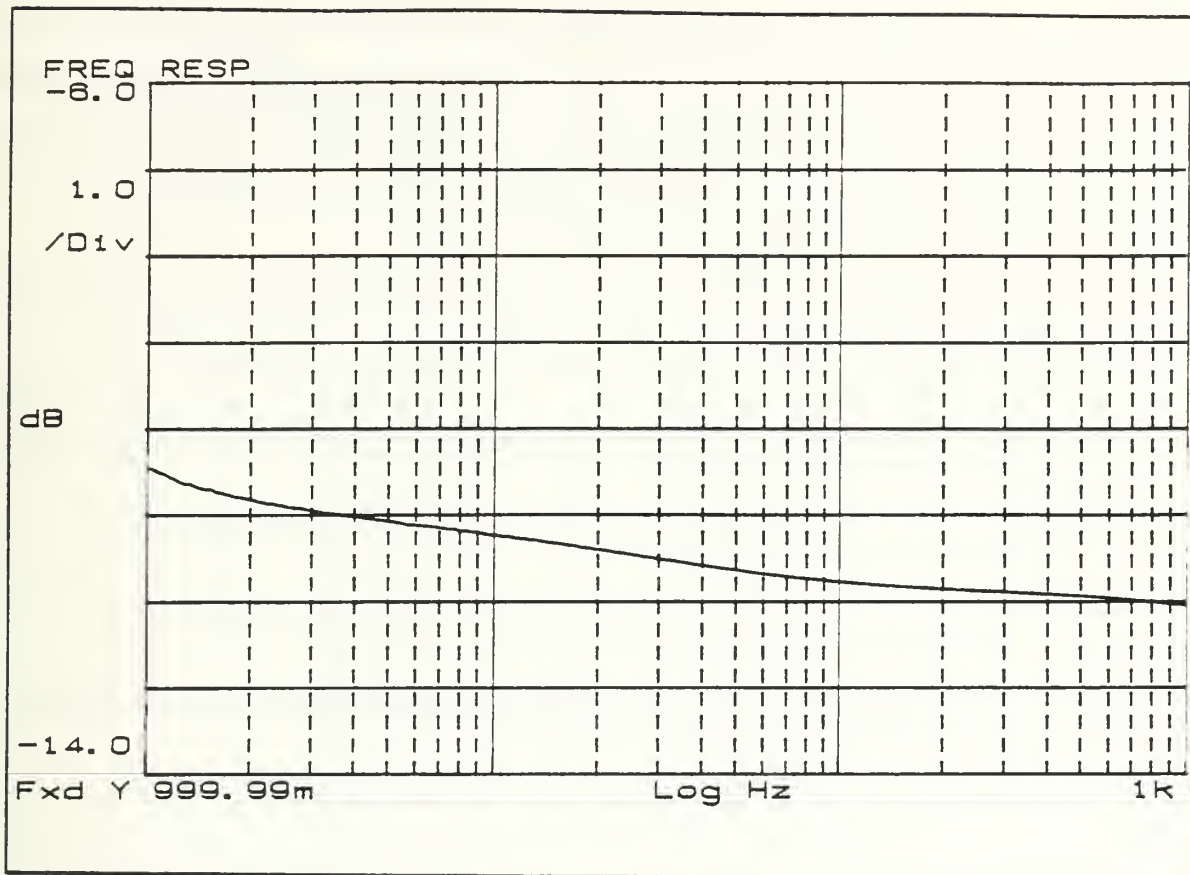


Figure 5.4 Frequency response of the piezoresistive microphone #2 with respect to the frequency response of the piezoelectric quartz microphone in low pressure helium.

The reader will note that the cavity effects occurring in low pressure air are not in evidence in low pressure helium.

If we subtract the curve at Figure 5.3, the response of the microphone #1 in low pressure helium, from the curve at Figure 5.1, the microphone #1 response in low pressure air, the result, shown at Figure 5.5, is the "pattern factor", described in Chapter II, of the cavity and piezoresistive microphone #1.

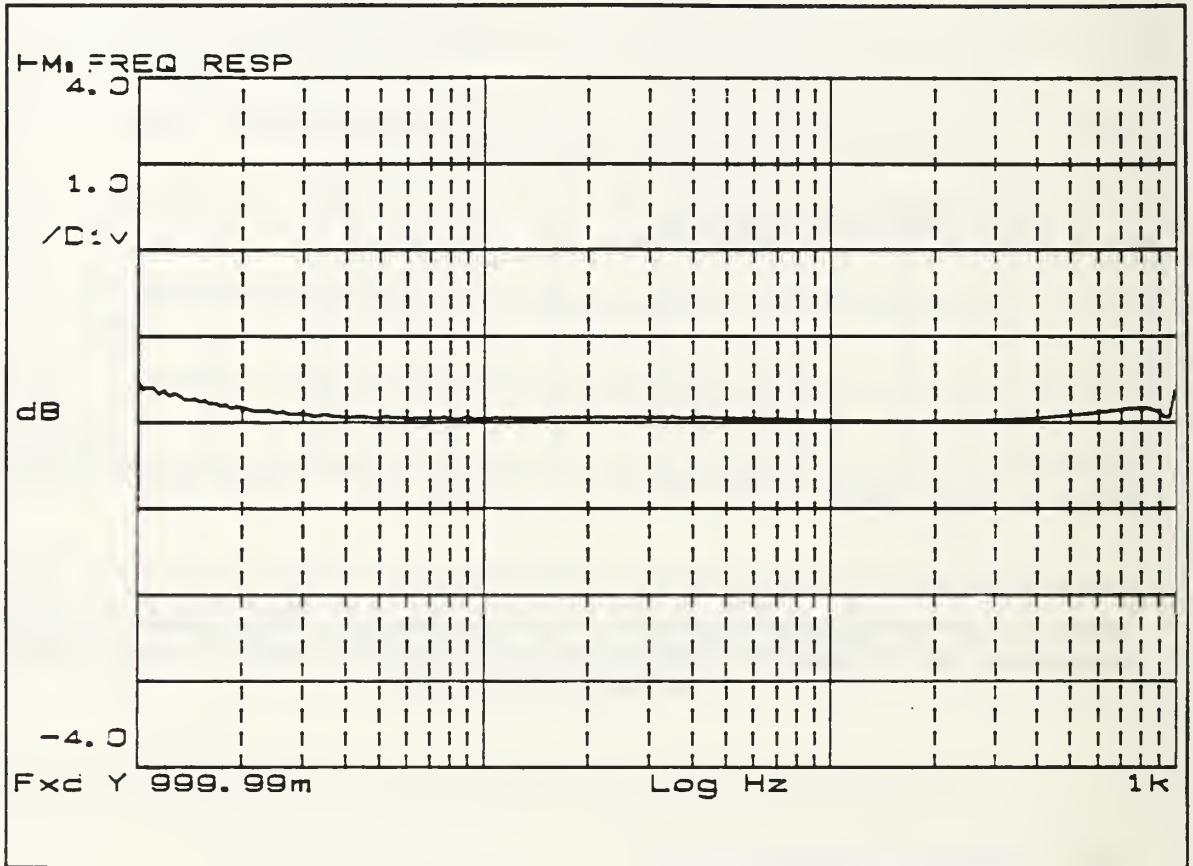


Figure 5.5 The "pattern factor" of piezoresistive microphone #1. Or, Frequency response of the piezoresistive microphone #1 in low pressure air with respect to the frequency response of the piezoresistive microphone #1 in low pressure helium.

Likewise, by subtracting the curve at Figure 5.4, the response of the microphone #2 in low pressure helium, from the curve at Figure 5.2, the microphone #2 response in low pressure air, the result, shown at Figure 5.6, is the "pattern factor", described in Chapter II, of the cavity and the piezoresistive microphone #2.

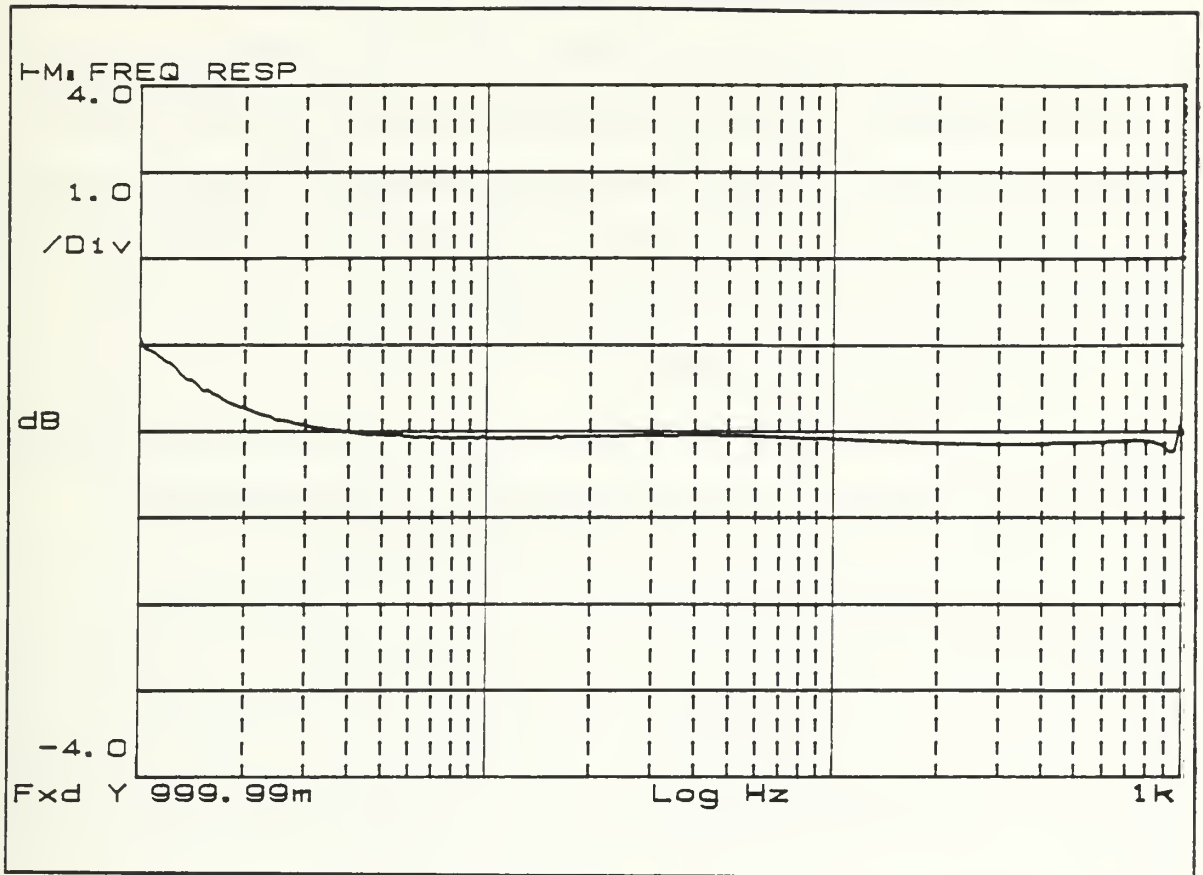


Figure 5.6 The "pattern factor" with piezoresistive microphone #2. Or, Frequency response of the piezoresistive microphone #2 in low pressure air with respect to the frequency response of the piezoresistive microphone #2 in low pressure helium.

The reader will note that between the frequency range from 50 to 300 Hz the "pattern factor" is unity (zero in decibels) as predicted by theory. Starting from about 300 Hz we begin to see the effects of the cavity resonance, but it occurs most significantly at around 800 Hz.

As well, starting from 50 Hz we begin to see another deviation from zero as we move to lower frequencies. This deviation cannot be attributed to cavity effects since these cannot occur at very low frequencies. I suspect that the effect of closing off the helium inside the apparatus (including the back volume of the driver) had the effect of increasing the sensitivity of the piezoelectric quartz microphone at low frequencies. The

back volume of the quartz microphone is coupled to the back volume of the driver through a capillary leak. Since the pressure has nowhere else to go if the apparatus is closed off, the pressure behind the driver will leak into the quartz microphone back volume and effectively increase the sensitivity. This increased sensitivity of the piezoelectric quartz microphone in low pressure helium conditions only will result in the "pattern factor" curve at Figures 5.5 and 5.6 to increase at very low frequencies.

c. High Pressure Helium

In helium at 132.5 psia, the response curve is shown at Figure 5.7 for the piezoresistive microphone #1 and Figure 5.8 for the piezoresistive microphone #2.

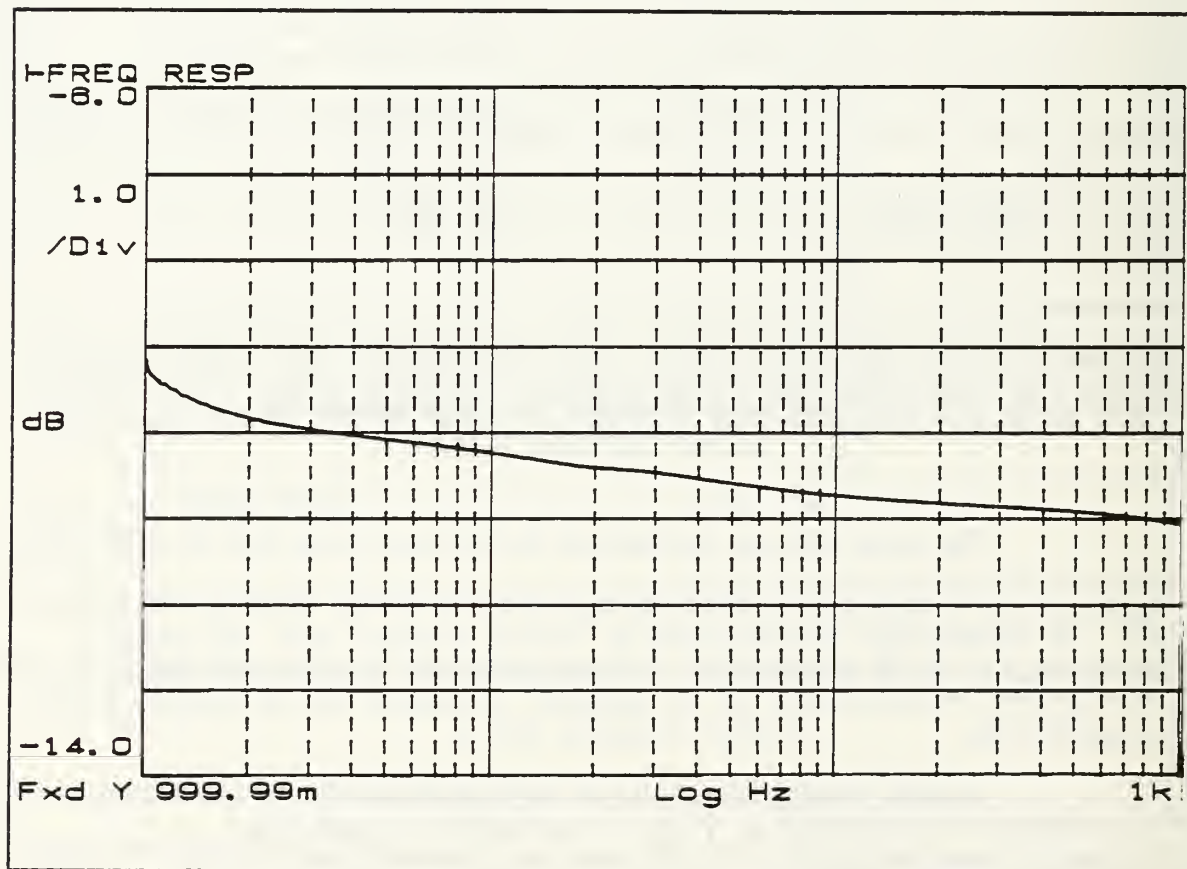


Figure 5.7 Frequency response of the piezoresistive microphone #1 with respect to the frequency response of the piezoelectric quartz microphone in high pressure helium.

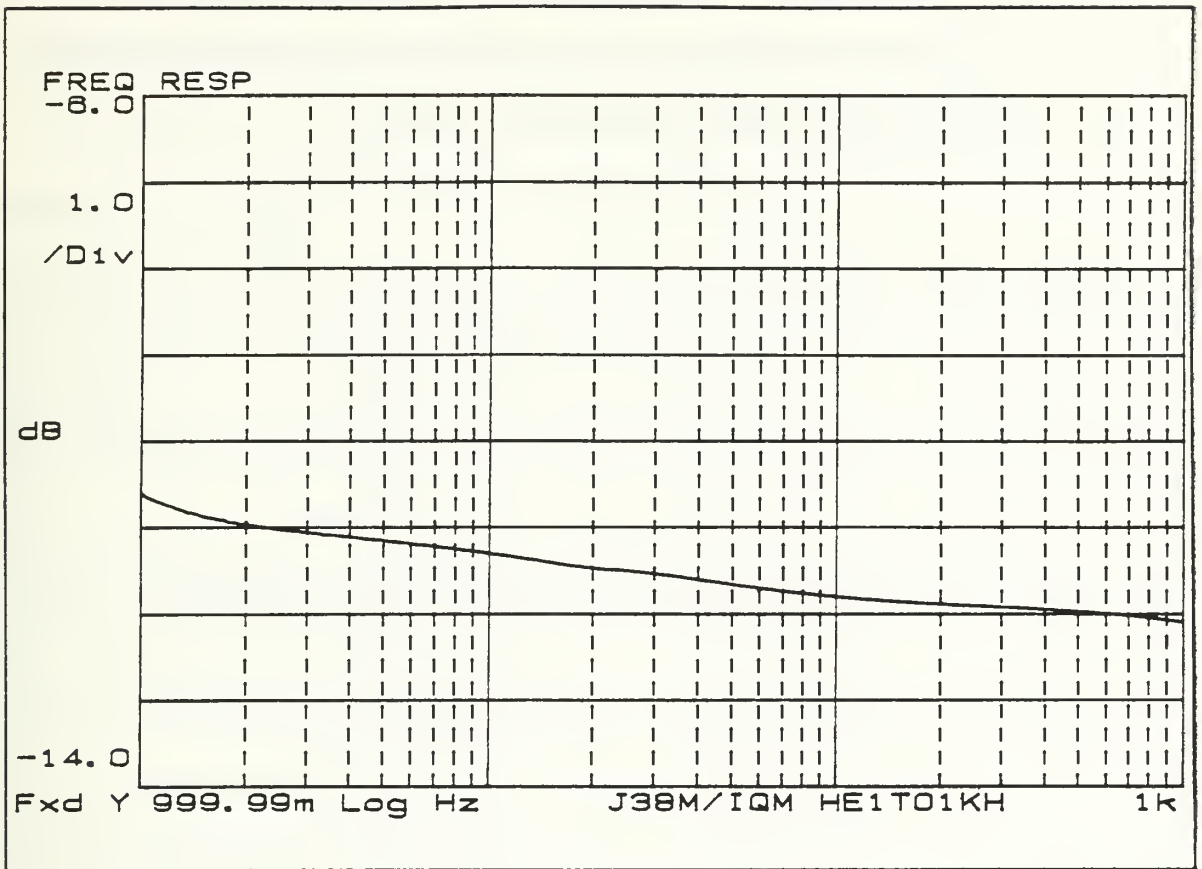


Figure 5.8 Frequency response of the piezoresistive microphone #2 with respect to the frequency response of the piezoelectric quartz microphone in high pressure helium.

By subtracting the curve Figure 5.7, the response of the microphone #1 in high pressure helium, from Figure 5.3, the response of microphone #1 in low pressure helium, we get a comparison between their responses, Figure 5.9.

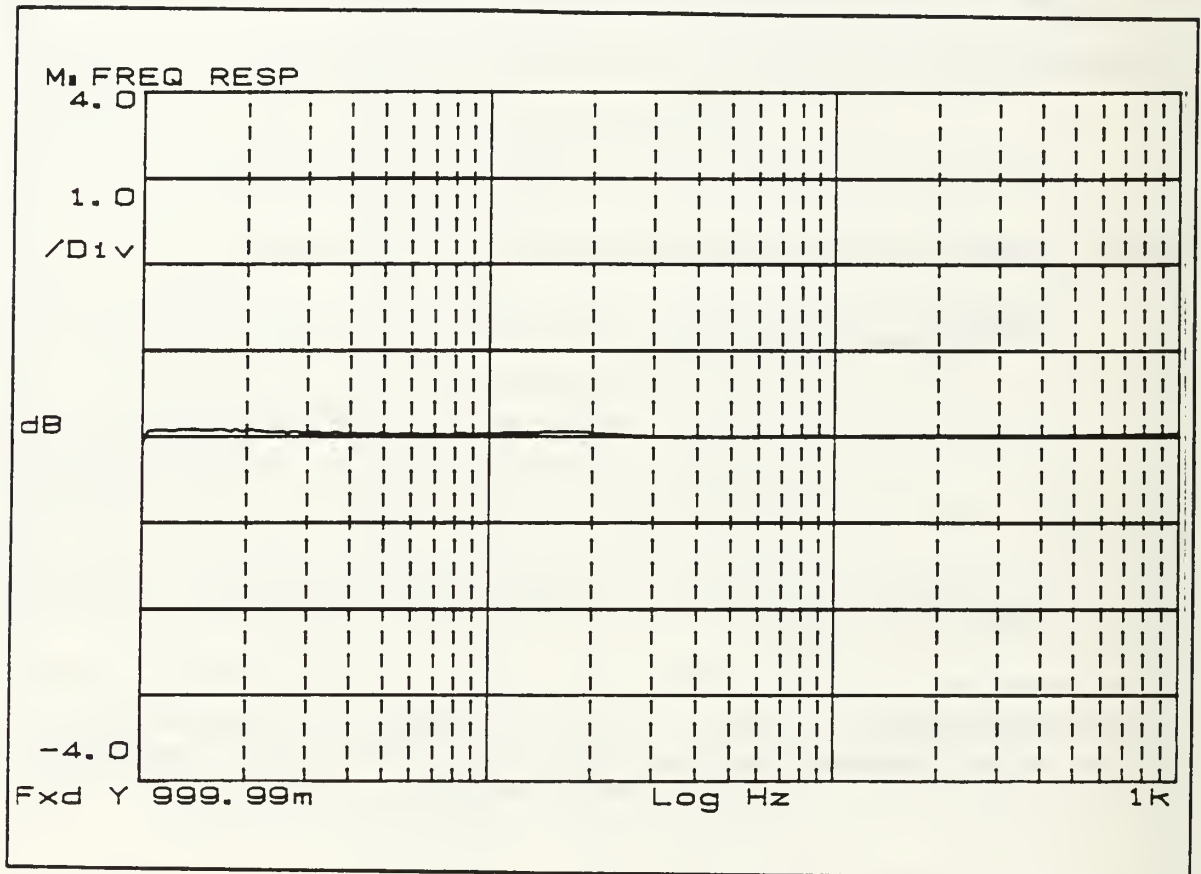


Figure 5.9 Comparison of the Frequency response of the piezoresistive microphone #1 in low pressure helium reference to its response in high pressure helium.

Similarly, by subtracting the curve Figure 5.8, the response of the microphone #2 in high pressure helium, from Figure 5.4, the response of microphone #2 in low pressure helium, we get a comparison between their responses, Figure 5.10.

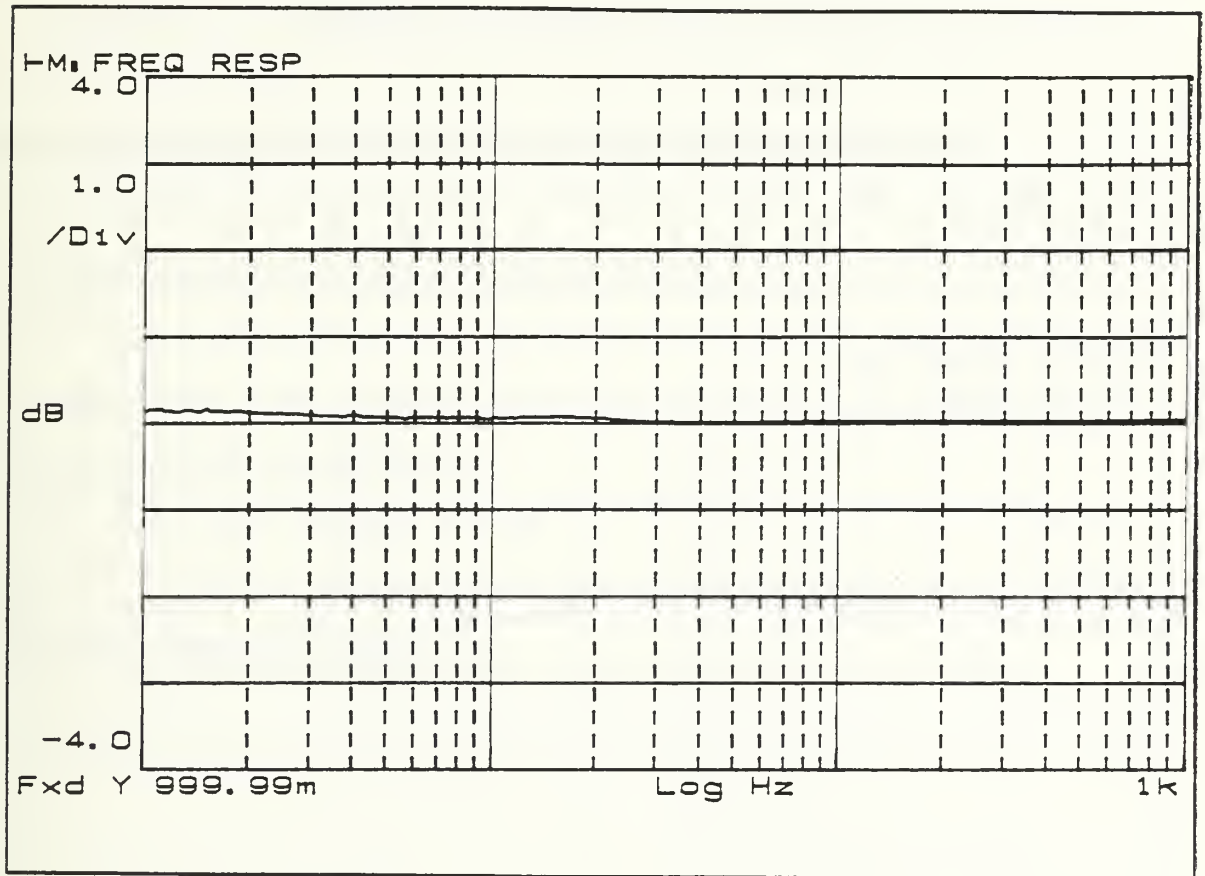


Figure 5.10 Comparison of the frequency response of the piezoresistive microphone #2 in low pressure helium reference to its response in high pressure helium.

Figure 5.9 and 5.10 show clearly that there is no significant difference between the piezoresistive microphone response in low or high pressure. This result suggests that a microphone calibration carried out at low pressures is equally valid under high pressure conditions.

2. Condenser Microphone Frequency Response

The results of this experiment are the responses of the 1/4" condenser microphone measured with respect to the piezoelectric quartz microphone at frequencies from 1 to 1000 Hz in the following media: low pressure air and low pressure helium.

a. Low Pressure Air

In low pressure air, the response curve for the 1/4" condenser microphone is shown at Figure 5.11.

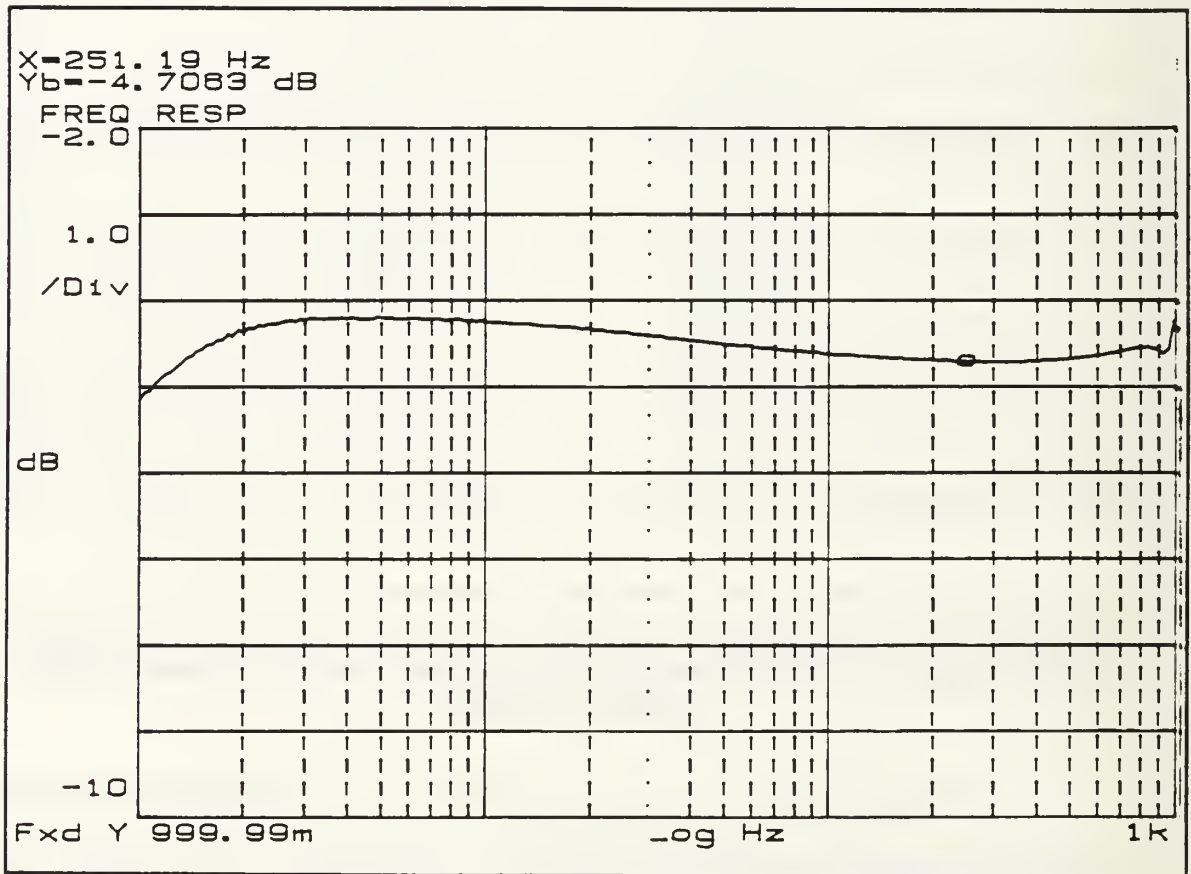


Figure 5.11 Frequency response of the 1/4" condenser microphone with respect to the frequency response of the piezoelectric quartz microphone in low pressure air.

The shape of the frequency response curve is, unfortunately, not as flat as I would like. This is due to a combination of several factors such as a non-flat response

from the piezoelectric quartz microphone, the low frequency roll off of the condenser microphone and its preamplifier, and cavity effects. The low frequency roll-off of the piezoelectric quartz microphone will account for the roll-off in Figure 5.11 below 5 Hz. The increase in response between 5 and 100 Hz is most likely due to the low frequency roll-off of the condenser microphone and its preamplifier. Below 5 Hz the condenser microphone roll-off becomes dominated by the piezoelectric quartz microphone roll-off and thus the decrease in response below 5 Hz. By generating the "pattern factor" curve for the condenser microphone we may show that the irregularity in the curve as we approach 900 Hz is a cavity effect. To produce the "pattern factor" we must generate the frequency response curve of the condenser microphone referenced to the piezoelectric quartz microphone in low pressure helium.

b. Low Pressure Helium

In low pressure helium, the response curve for the 1/4" condenser microphone is shown at Figure 5.12.

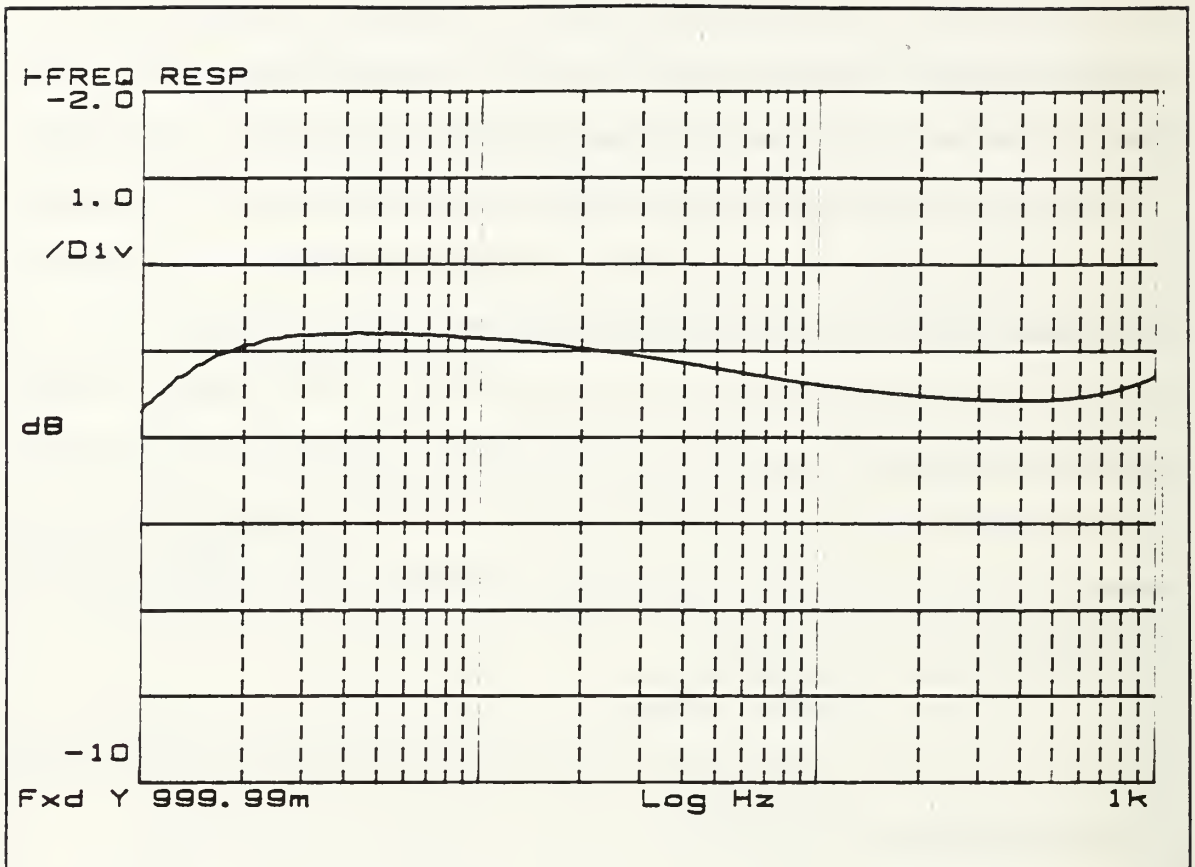


Figure 5.12 Frequency response of the 1/4" condenser microphone with respect to the frequency response of the piezoelectric quartz microphone in low pressure helium.

By subtracting the curve at Figure 5.12, the response of the 1/4" condenser microphone in low pressure helium, from the curve at Figure 5.11, the response of the 1/4" condenser microphone in low pressure air, the result, shown at Figure 5.13, is the "pattern factor" of the condenser microphone.

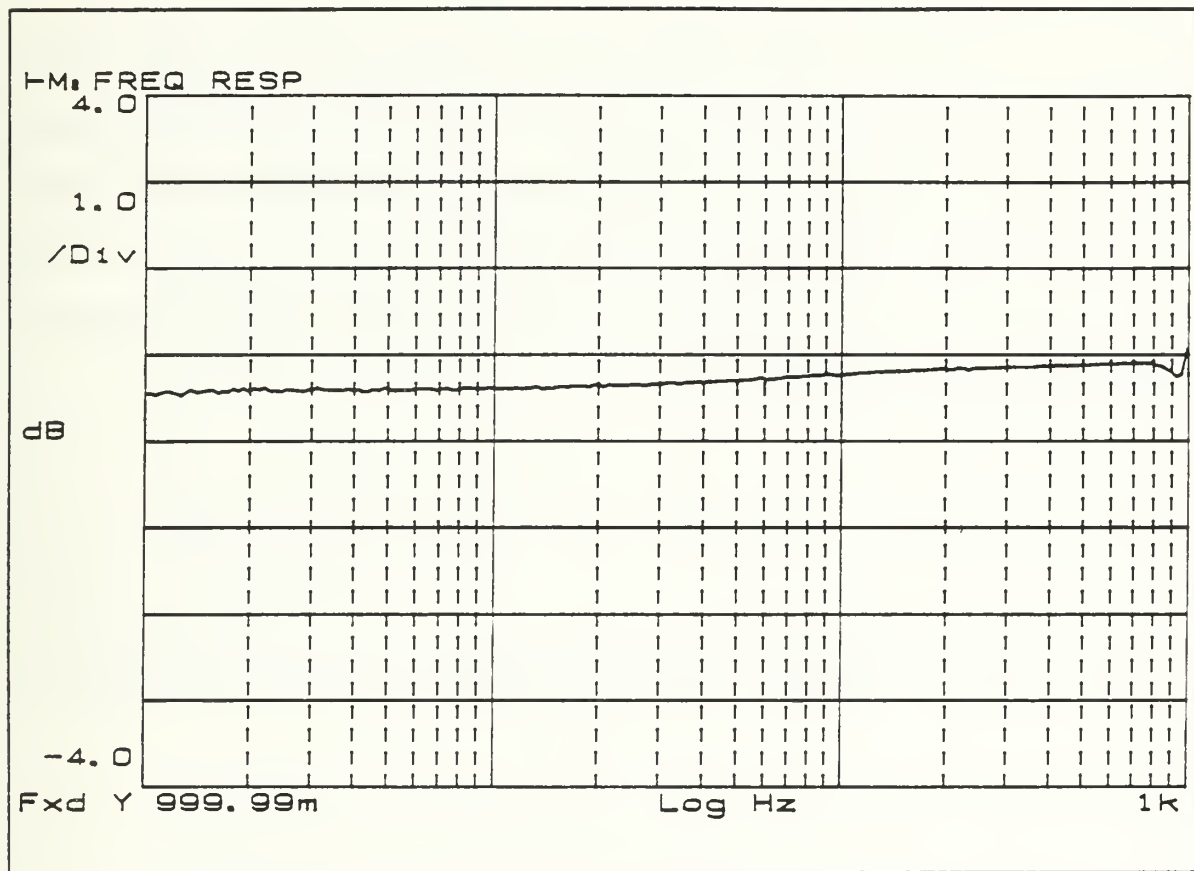


Figure 5.13 The "pattern factor" with the condenser microphone.

The cavity resonance occurring at approximately 900 Hz shows up clearly in the curve for the "pattern factor." Returning to Figure 5.11, we can now explain the irregularity in the curve as we approach 900 Hz as a cavity effect and not a microphone effect. There are, however, two discrepancies which are clearly amiss with Figure 5.13. The first is that nowhere along the curve does the "pattern factor" equal zero as predicted, and the second is the apparent slope between 50 and 500 Hz. There is no low frequency

rise in the curve similar to that in Figures 5.5 and 5.6 since the back volume of the driver was not closed off to seal in helium and was left open to the ambient pressure.

Except then for factors independent of the condenser microphone itself, we can convince ourselves that the frequency response of the condenser microphone is "flat" in the range of interest.

We may now begin to determine the calibration curve for the piezoresistive microphones by subtracting the curve at Figure 5.11, the response of the 1/4" condenser microphone in low pressure air, from the curve at Figure 5.1, the microphone #1 response in low pressure air. The result is the frequency response curve for the piezoresistive microphone, with respect to the frequency response of the 1/4" condenser microphone in low pressure air, shown at Figure 5.14.

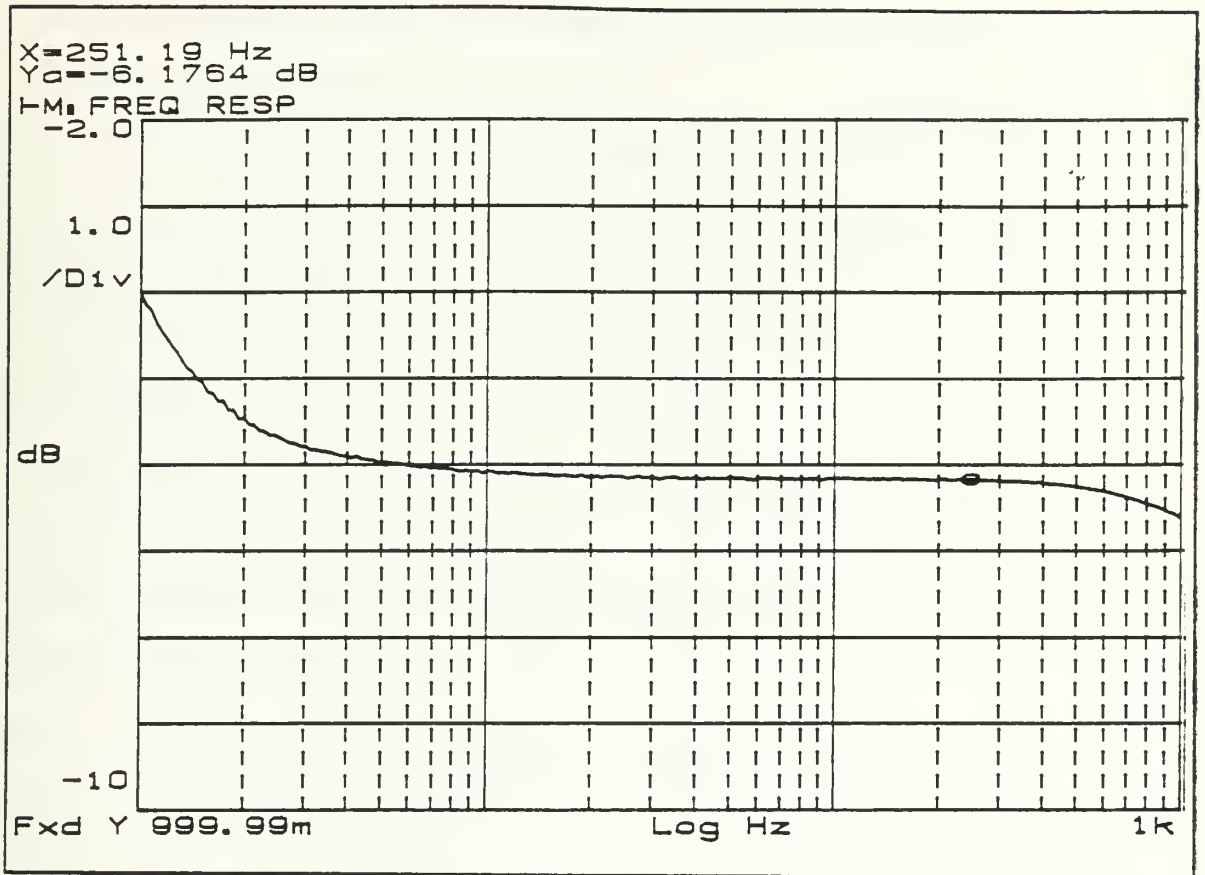


Figure 5.14 Frequency response of the piezoresistive microphone #1 with respect to the frequency response of the 1/4" condenser microphone in low pressure air.

Likewise, by subtracting the curve at Figure 5.11, the response of the 1/4" condenser microphone in low pressure air, from the curve at Figure 5.2, the microphone #2 response in low pressure air, the result is the frequency response curve for the piezoresistive microphone, with respect to the frequency response of the 1/4" condenser microphone in low pressure air, shown at Figure 5.15.

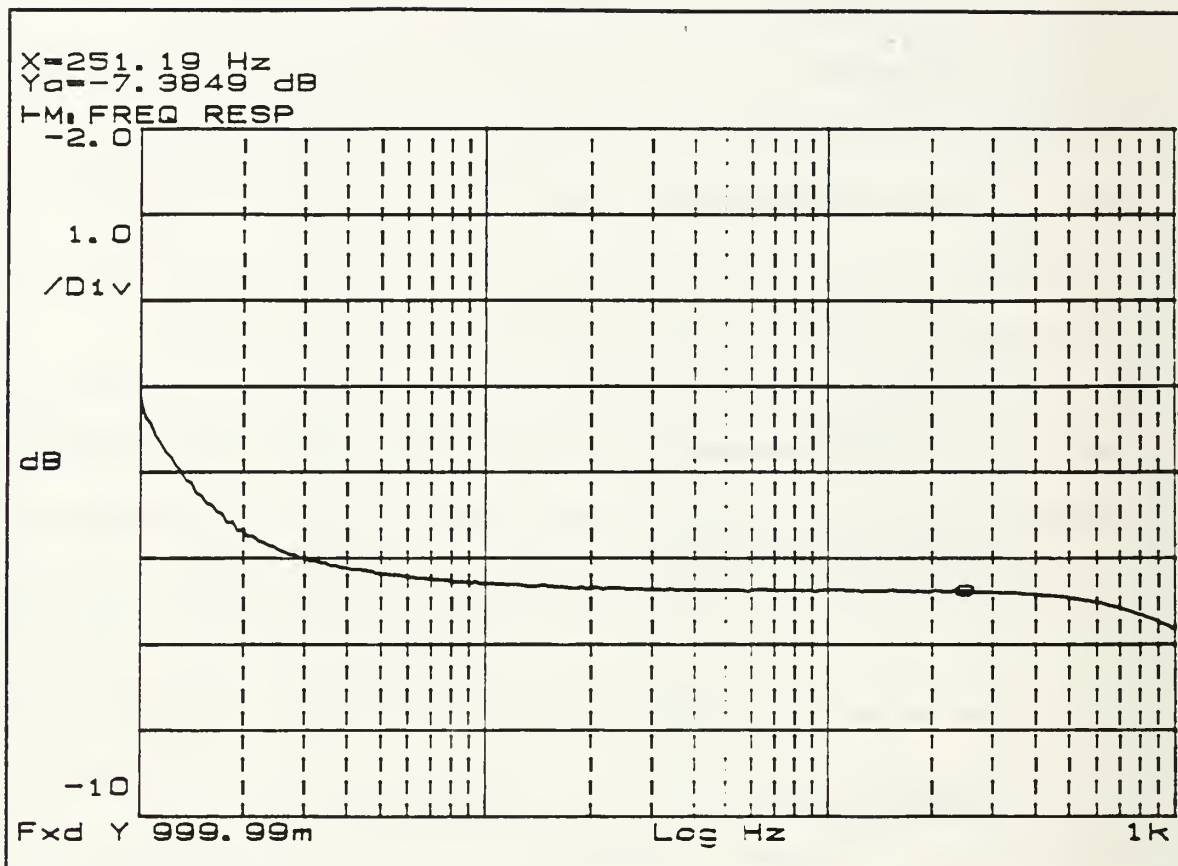


Figure 5.15 Frequency response of the piezoresistive microphone #2 with respect to the frequency response of the 1/4" condenser microphone in low pressure air.

The results of Figure 5.14 and Figure 5.15 show the calibration curve of the piezoresistive microphones with respect to the frequency response of the 1/4" condenser microphone. To relate these results back to our theory in Chapter II, these two curves in Figures 5.14 and 5.15, represent the values for $20 \text{ Log } \frac{V_x}{V_A}$ from equation 2.7. Thus, these two curves will form the basis for my comparison calibration for the two piezoresistive microphones. We need now only to determine the calibration curve of the condenser microphone (the value $20 \text{ log } M_A$ from equation 2.7) to determine the calibration of the piezoresistive microphones. The calibration curve of the condenser microphone is conveniently supplied by the microphone manufacturer. However, in order to convince

myself that it is, in fact, correct, I have carried out my own calibration using a pistonphone device described in the Chapter III of this thesis.

3. Condenser Microphone Calibration

Although the calibration of the condenser microphone is known from the manufacturers specifications, it is useful to confirm the validity of the calibration by using the pistonphone. The voltage output of the microphone securely seated in the pistonphone was measured to be 121.16 mV rms with an uncertainty of less than 0.1 %. The nominal Sound Pressure Level in the pistonphone is 124.08 dB plus a correction for barometric pressure of +0.04 dB gives a Sound Pressure Level of 124.12 dB re 20 μ Pa. The uncertainty in this value is given by the manufacturer as ± 0.12 %. Thus, the sensitivity of the microphone at 251.2 Hz is

$$M_A = \frac{V}{P} = \frac{121.16 \text{ mV}}{10^{\left(\frac{124.12}{20}\right)} 20 \times 10^{-6} \text{ Pa}} = 3.770 \text{ mV/Pa} = -48.47 \text{ dB re 1 V/Pa} \quad (5.1)$$

By taking the square root of the sum of the squares of the uncertainties we can determine the overall uncertainty in M_A as ± 0.16 %. The sensitivity given by the manufacturer for this frequency is -49.0 dB re 1 V/Pa which is reasonably close to my value. However, since my calibration is the most recent I have redefined the manufacturers condenser microphone calibration curve, Figure 5.16, to fit the new value for sensitivity at 251.2 Hz. The zero decibel point on the vertical axis corresponds to the new sensitivity of -48.47 dB re 1 V/Pa.

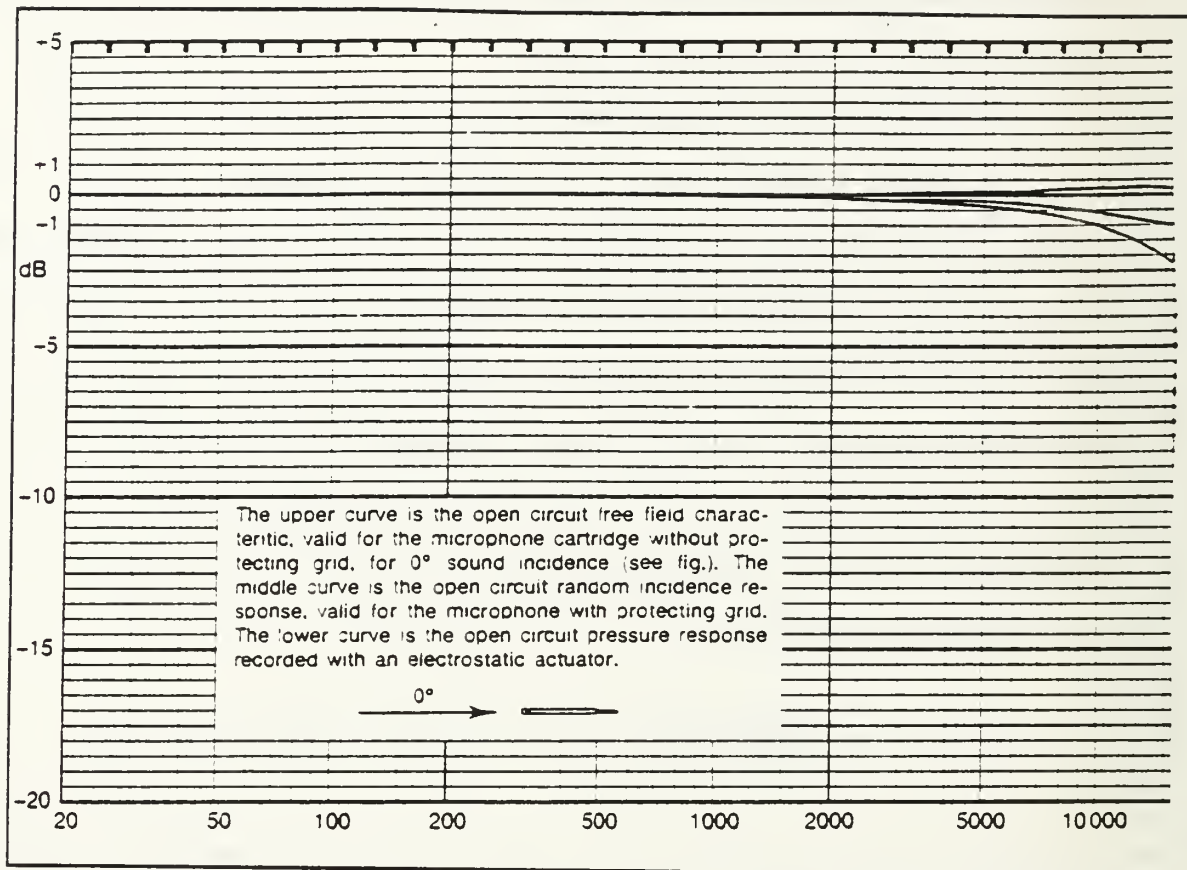


Figure 5.16 Newly calibrated manufacturers calibration chart for the 1/4" condenser microphone.

4. Piezoresistive Microphone Calibration

The calibration of the piezoresistive microphones can now be determined in accordance with equation 2.7:

$$20 \text{ Log } M_x = 20 \text{ Log } M_A + 20 \text{ Log } \frac{V_x}{V_A} \quad (5.2)$$

The values for $20 \text{ Log } \frac{V_x}{V_A}$ for the piezoresistive microphone #1 come from Figure 5.14. Its value at 251 Hz which lies on the "flat" region of the curve is -6.18 dB. To determine the uncertainty in this value I conducted a test of the dynamic signal analyzer where the output was simultaneously connected to channel 1 and channel 2 of the analyzer.

any deviation from zero would indicate the error in the machine. I determined the error through this test to be about ± 0.005 dB which for the purposes of these calculations is negligible.

Taking into account the pre-amplifier gain on the piezoelectric microphone #1 of 40.01 dB, gives a value for $20 \text{ Log } \frac{V_X}{V_A}$ of -46.19 dB. The values for $20 \text{ log } M_A$, from Figure 5.16, is -48.47 dB. Therefore, we add Figure 5.14 to Figure 5.16 and the result will be the calibration curve for the piezoresistive microphone #1 shown in Figure 5.17. Mathematically,

$$20 \text{ Log } M_X = -48.47 - 46.19 = -94.66 \text{ dB} \quad (5.3)$$

Converting the decibel value of the sensitivity in the "flat" region to a value in volts/psi gives

$$M_X = 127.5 \text{ mV/psi} \quad (5.4)$$

with an uncertainty of $\pm 0.16\%$.

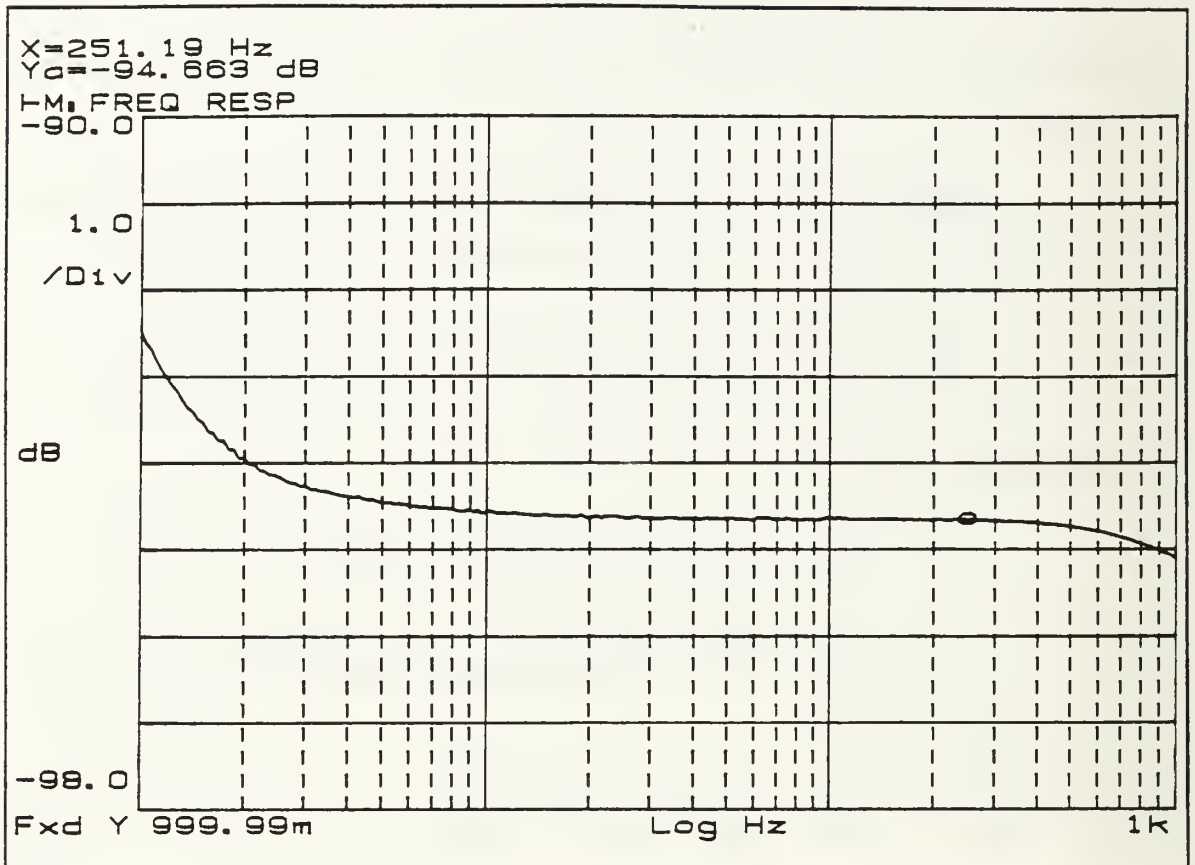


Figure 5.17 Calibration curve for the piezoresistive microphone #1.

Similarly, the values for $20 \text{ Log } \frac{V_X}{V_A}$ for the piezoresistive microphone #2 come from Figures 5.15. Its value at 251 Hz which lies on the "flat" region of the curve is -7.38 dB with an uncertainty which I have determined to be negligible. Taking into account the pre-amplifier gain on the piezoelectric microphone #2 of 40.01 dB, gives a value for $20 \text{ Log } \frac{V_X}{V_A}$ of -47.39 dB. Thus, adding Figure 5.15 to Figure 5.16 will result in the calibration curve for the piezoresistive microphone #2 shown in Figure 5.18. Mathematically,

$$20 \text{ Log } M_x = -48.47 - 47.39 = -95.86 \text{ dB} \quad (5.5)$$

Converting the decibel value of the sensitivity in the "flat" region to a value in volts/psi gives

$$M_X = 111.05 \text{ mV/psi} \quad (5.6)$$

with an uncertainty of $\pm 0.16\%$.

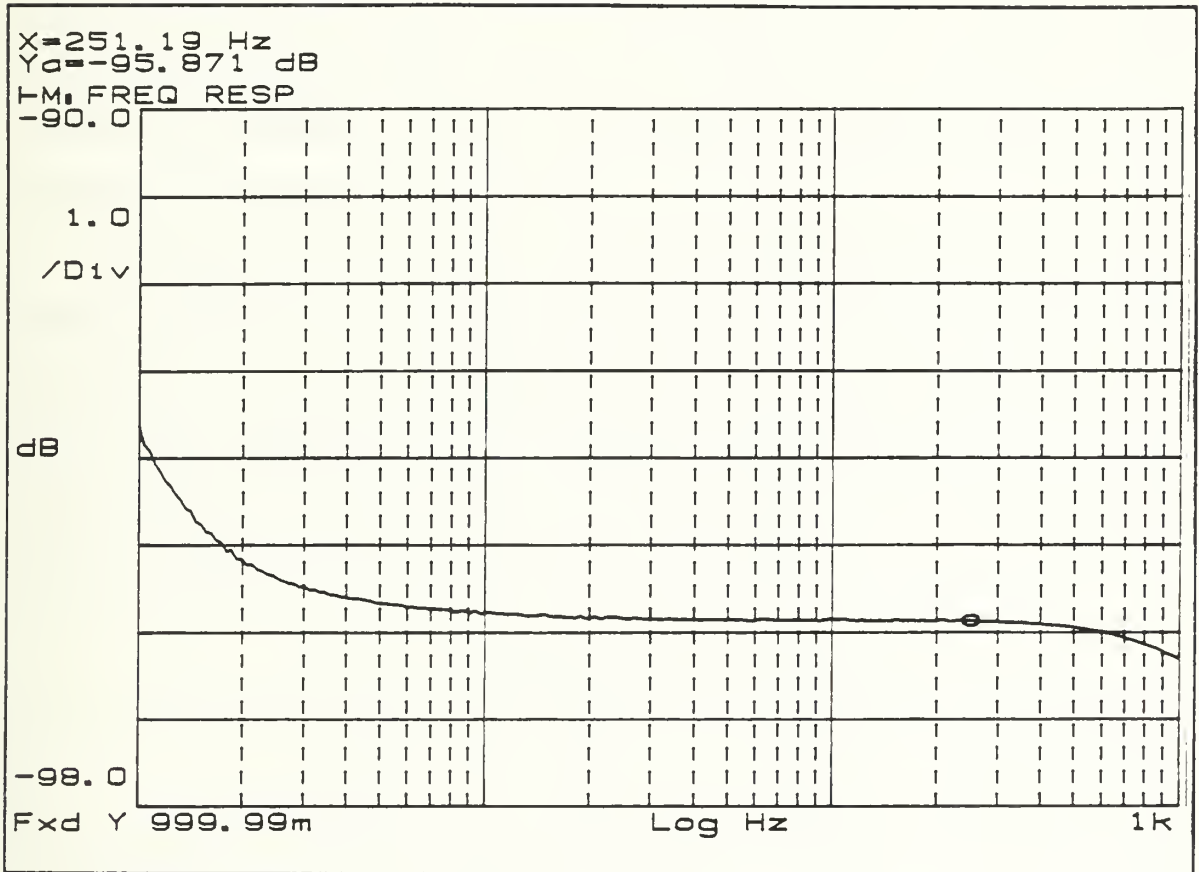


Figure 5.18 Calibration curve for the piezoresistive microphone #2.

The results of this chapter can be summarized as follows: The frequency response of the two piezoelectric microphones and the condenser microphone were recorded with respect to the piezoelectric quartz microphone. I was able to identify the low frequency roll-off effects as well as the cavity effects of each of these curves and either

rationalize or eliminate them. The final result is a calibration curve for the two piezoresistive microphones that is valid above the low frequency roll-off of the condenser microphone.

VI. CONCLUSIONS

The purpose of this thesis is to provide a calibration of two piezoresistive microphones by comparison with a high quality commercially available condenser microphone. There were two calibrations carried out; the first was a static calibration test, and the second was a dynamic calibration test. The static calibration determined the sensitivity, M_X , of the two piezoresistive microphones under static pressure conditions. The dynamic calibration determined the calibration curve of the two piezoresistive microphones with respect to a condenser microphone of known calibration.

If we extrapolate the "flat" region of the piezoresistive calibration curves determined in Figure 5.17 and Figure 5.18 to the left all the way to zero Hz or static pressure then value of sensitivity at 251.2 Hz should coincide with the value determined during the static tests. Table 6.1 below summarizes the values of sensitivity for each piezoresistive microphone at static and dynamic pressure and their relative difference and as well provides the Original Equipment Manufacturers (OEM) specifications for comparison.

TABLE 6.1 SUMMARY OF RESULTS.

	Static Sensitivity (mV/psi)	Dynamic Sensitivity (mV/psi)	OEMs Sensitivity (mV/psi)	Difference between static and dynamic
Piezoresistive Microphone #1	$125.9 \pm 0.1\%$	$127.5 \pm 0.16\%$	125.8	1.3%
Piezoresistive Microphone #2	$110.6 \pm 0.1\%$	$111.1 \pm 0.16\%$	111.1	0.4%

Thus, within an uncertainty of about $0.1\% + 0.16\% = 0.26\%$, I should be able to conclude that the "flat" region of the calibration curve extends from static pressures to about 250 Hz. However, for the piezoelectric microphone #1, I measured a 1.3 % difference

between the static value of sensitivity and the dynamic value at 251.2 Hz, and for the piezoelectric microphone #2, I measured this difference to be 0.4%. These values fall outside the range of uncertainty and I cannot account for the differences.

If I ignore the low frequency roll-off of the condenser microphone and extrapolate the "flat" region of the calibration curves (Figures 5.17 and 5.18) for the two piezoresistive microphones to zero Hz, I am able to generate an absolute calibration curve for the two piezoresistive microphones in Figures 6.1 and 6.2 below.

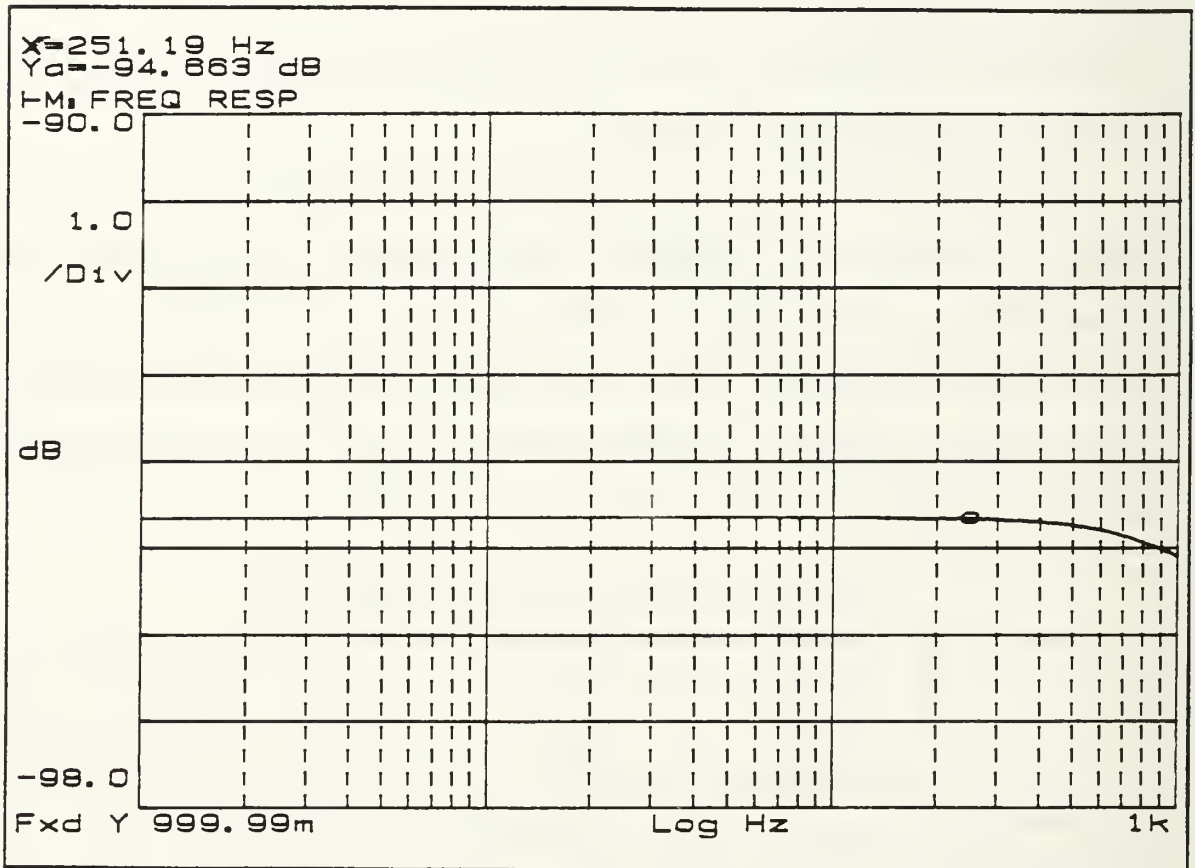


Figure 6.1 Absolute calibration of the piezoresistive microphone #1.

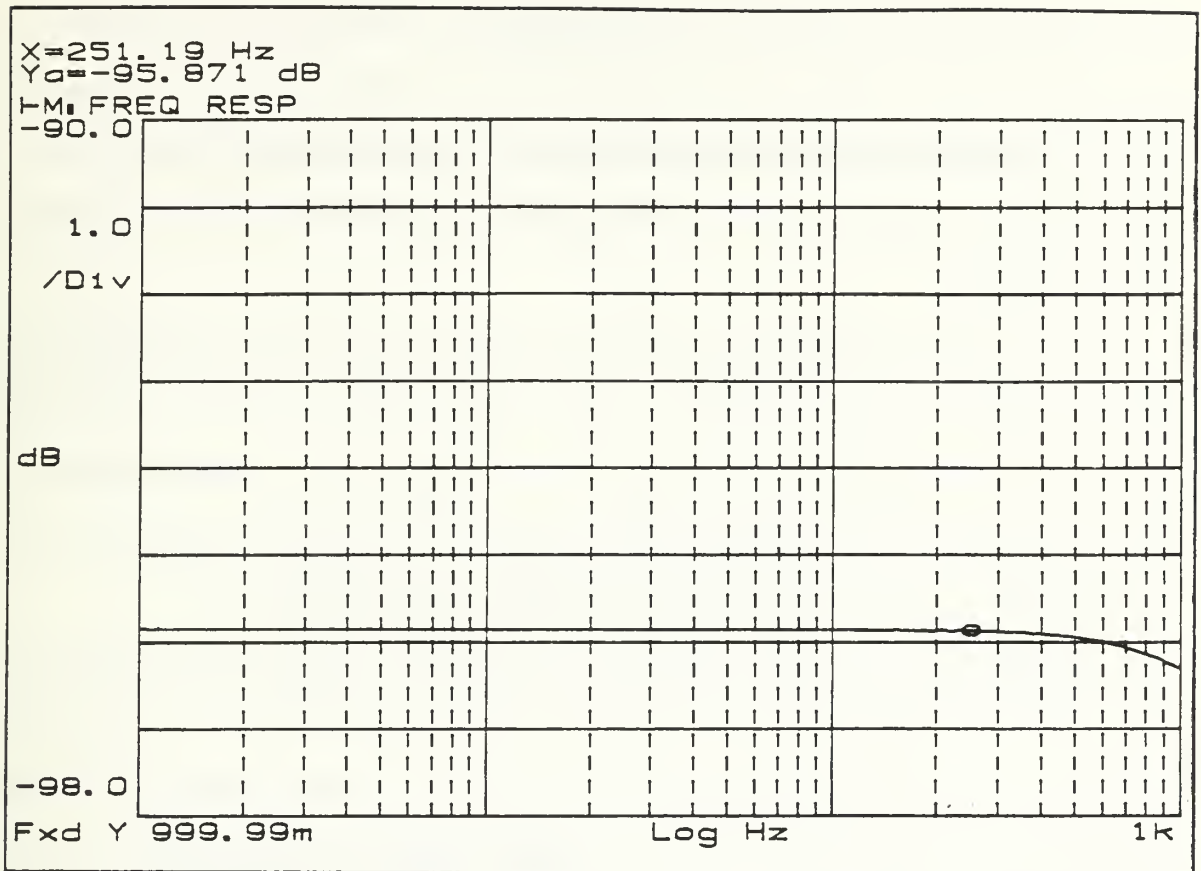


Figure 6.2 Absolute calibration of the piezoresistive microphone #2.

We are most concerned with the frequency range of normal thermoacoustic refrigerator operation between 400 and 600 Hz. The piezoresistive microphones, although they are "flat" at low frequencies begin to deviate from this "flatness" at frequencies greater than about 300 Hz.

From the calibration curves Figure 6.1, the response in the range between 400 and 600 Hz is -94.69 to -94.79 dB for the piezoresistive microphone #1. The worst case error between these values and the static sensitivity for the piezoresistive microphone #1, from equation 5.3, is 0.11 dB or 1.2%.

Similarly, from the calibration curves Figure 6.2, the response in this same range is -95.90 to -96.00 dB for the piezoresistive microphone #2. The worst case error between

this value and the static sensitivity for the piezoresistive microphone #2, from equation 5.4, is 0.08 dB or 0.2%. These calculations show that the difference between the static and dynamic calibrations getting smaller as we move out to higher frequencies. This is due to the sensitivity in figures 6.1 and 6.2 declining in this region and approaching the value of static sensitivity.

If we return to the original aim of the thesis which was to produce a calibration with 1% uncertainty, it is clear from Table 6.1 that I can meet this aim. As well, I can also claim that within the same level of uncertainty, the static sensitivity is a good value for the dynamic sensitivity in the low frequency "flat " region for piezoresistive microphone #2. I cannot, however, make the same claim for piezoresistive microphone #1.

I, therefore, recommend using the static sensitivity as a good value of sensitivity below 600 Hz for the piezoresistive microphone #2. As well, I recommend using the static sensitivity as an approximation for the values of sensitivity below 600 Hz for piezoresistive microphone #1. For truly accurate values of the sensitivity, however, I recommend using the dynamic calibration curves at Figures 6.1 and 6.2.

I recommend that if future calibrations are to be made, consideration be given to recording the free field frequency response of the microphones in an anechoic chamber. This would free the experiment from any possible cavity effects in order to ascertain the true shape of the calibration curve. I also recommend that the device for attaching the condenser microphone to the dynamic pressure vessel be improved such that the pressure sensing face of the microphone can be placed in exactly the same position as the pressure sensing face of the piezoresistive microphones. Obviously, in order to have a valid calibration it is important that the conditions under which the microphones are compared are exactly the same and this includes the position of the pressure sensing face of each microphones with respect to the cavity.

APPENDIX A

In this appendix, I present the schematic diagrams of the home-made preamplifier used with the piezoresistive microphones in figures A.1, A.2, and A.3.

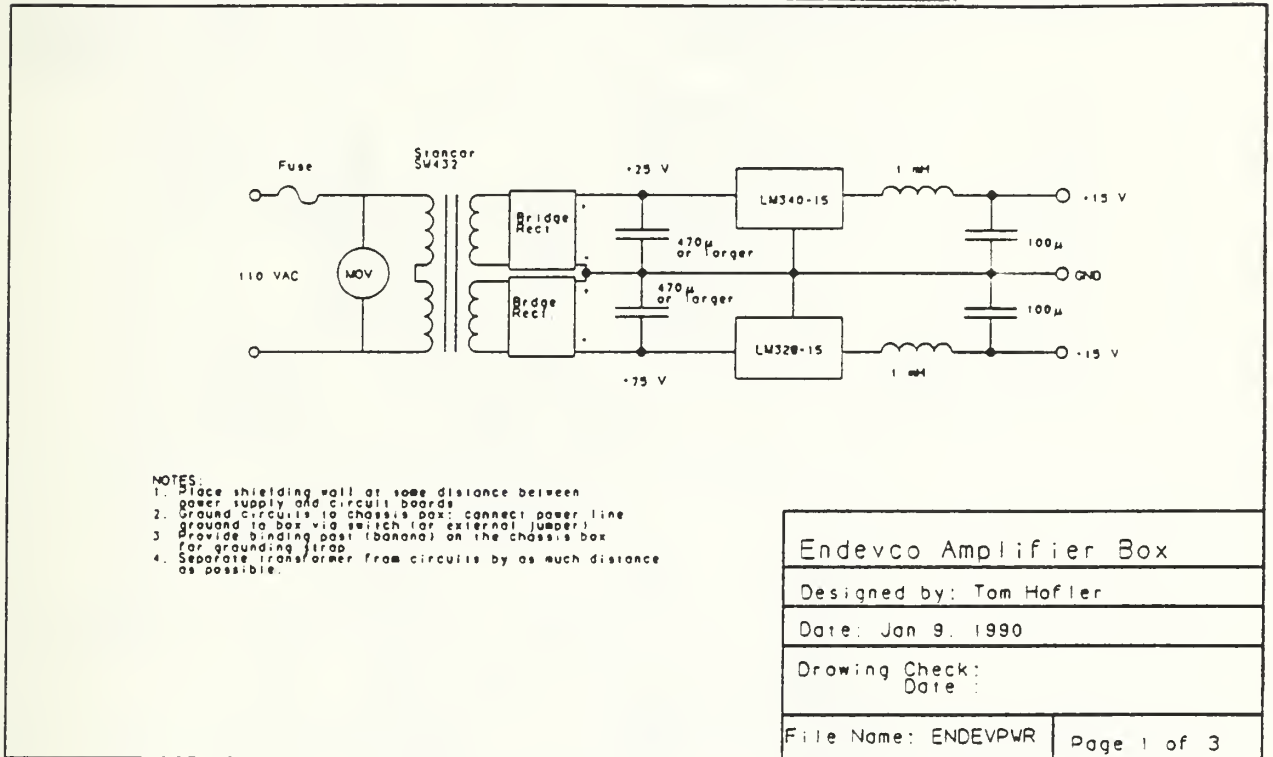
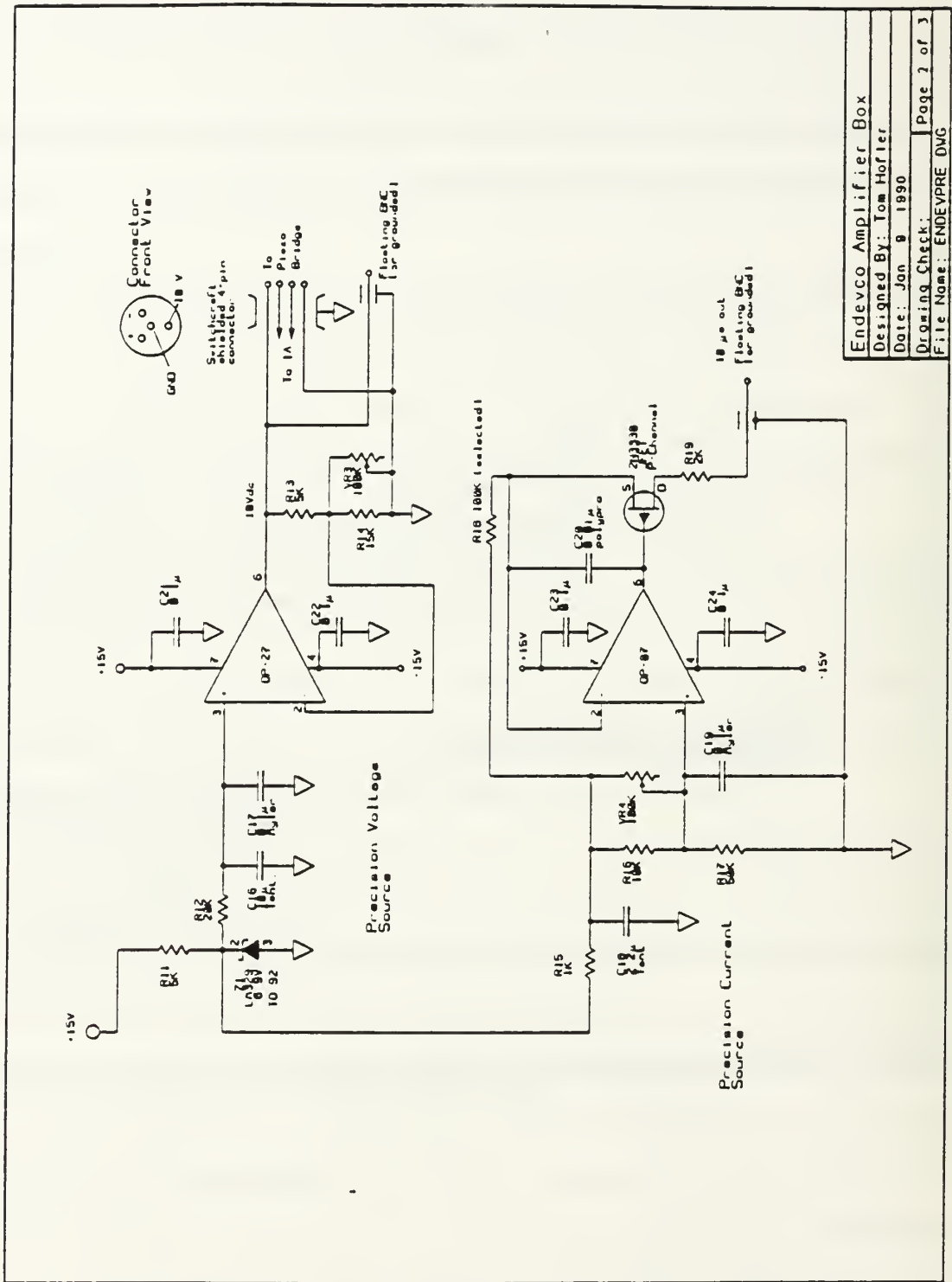


Figure A.1 Schematic Diagram of Piezoresistive Microphone Preamplifier, Drawing 1 of 3.



Endevco Amplifier Box
 Designed By: Tom Hofter
 Date: Jan 9 1990
 Drawing Check: _____ Page 2 of 3
 File Name: ENDEVPRE.DWG

Figure A.2 Schematic Diagram of Piezoresistive Microphone Preamplifier, Drawing 2 of 3.

LIST OF REFERENCES

1. T. Hofler, J. Acoust. Soc. Am. **83** (2), 777 (1988).
2. Endevco Corp., San Juan Capistrano, CA 92675, microphone model 8510B-2, Serial No.A13N; and Endevco microphone model 8510B-2, Serial No. J38M.
3. Brüel & Kjaer Instruments Inc., DK-2850 Nærum, Denmark, 1/4" microphone type 4135, Serial No.1518317.
4. Kinsler, Frey, Coppens, and Sanders, *Fundamentals of Acoustic* (Wiley New York, 1982), Sec. 14.13 and Chap. 14.
5. L. L. Beranek, *Acoustic Measurements* (American Institute of Physics 1988), Sec. 4.2 and Chap. 4.
6. Brüel & Kjaer Instruments Inc., DK-2850 Nærum, Denmark, pistonphone type 4228.
7. Emerson & Cuming, Inc., Canton, MA 02021, Stycast 2850.
8. Emerson & Cuming, Inc., Canton, MA 02021, Stycast 1266.
9. Brüel & Kjaer Instruments Inc., DK-2850 Nærum, Denmark, Microphone power supply type 2807.
10. Brüel & Kjaer Instruments Inc., DK-2850 Nærum, Denmark, pre-amplifier type 2639.
11. Phillips Co., 9200 Den Der Monde, Belgium, 1" dome loudspeaker model no. AD 0162 T8.

12. Dow Corning Corp., Midland, MI 48640, 732 RTV adhesive.
13. MKS Instruments, Inc., Burlington, MA 01803, MKS Baratron Pressure Head Type 310H-1000, Serial No. 22573-1.
14. MKS Instruments, Inc., Burlington, MA 01803, MKS Baratron Electronic Display Unit Type 270, Serial No. 22573-1.
15. Hewlett-Packard Co., Palo Alto, CA 94304, Multimeter, model 3478A.
16. Hewlett-Packard Co., Palo Alto, CA 94304, Dynamic Signal Analyzer, model 3562A.
17. Hewlett-Packard Co., Palo Alto, CA 94304, DC Power Supply Amplifier, model 6824A.
18. John Fluke Mfg. Co., Inc., Everett, Washington, Multimeter model 75.
19. Ithaco Inc., Ithaca, NY 14850, Low Noise Preamplifier model 1201.
20. Hewlett-Packard Co., Palo Alto, CA 94304, Plotter, model 7470A.
21. Hewlett-Packard Co., Palo Alto, CA 94304, Disk Drive, model 9129.
22. Endevco Corp., San Juan Capistrano, CA 92675, microphone model 8510B-2, Serial No. A13N.
23. Endevco Corp., San Juan Capistrano, CA 92675, microphone model 8510B-2, Serial No. J38M.

INITIAL DISTRIBUTION LIST

	No. of Copies
1. Prof. T. J. Hofler Physics Department, (Code PH/Hf) Naval Postgraduate School Monterey, CA 93943	3
2. Prof. S. L. Garrett Physics Department, (Code PH/Gx) Naval Postgraduate School Monterey, CA 93943	2
3. Director of Maritime Aircraft Engineering and Maintenance ATTN: Capt R.J. Stockermans, DMAEM 4-2 Bldg 155, CFB Ottawa (North) Ottawa, Ontario Canada K1A 0K4	2
4. Library, Code 52 Naval Postgraduate School Monterey, CA 93943-5002	2
5. Defense Technical Information Center Cameron Station Alexandria, VA 22304-6145	2
6. Mr. Tom Kaweck NRL, Concept Development Code 8240 4555 Overlook Ave. Washington, DC 20375-5000	1
7. Mr. Phil Green Naval Research Laboratory Code 9120 4555 Overlook Ave. Washington, DC 20375-5000	1
8. Mr. Joe Mims GE Government Services 1050 Bay Area Blvd. Houston, TX 77058	1
9. Prof. A. A. Atchley Physics Dept (Code PH/Ay) Naval Postgraduate School Monterey, CA 93943	1

846-217

Thesis
S7315 Stockermans
c.1 Comparison calibration
of piezoresistive micro-
phones for acoustic power
measurements.

Thesis
S7315 Stockermans
c.1 Comparison calibration
of piezoresistive micro-
phones for acoustic power
measurements.



DUDLEY KNOX LIBRARY



3 2768 00036327 9